Polyelectrolytes

International Edition: DOI: 10.1002/anie.201710272
German Edition: DOI: 10.1002/ange.201710272

Porous Polyelectrolytes: The Interplay of Charge and Pores for New Functionalities

Weiyi Zhang, Qiang Zhao, and Jiayin Yuan**

Keywords:
energy conversion · environmental chemistry · medicinal chemistry · porous polyelectrolytes · smart materials

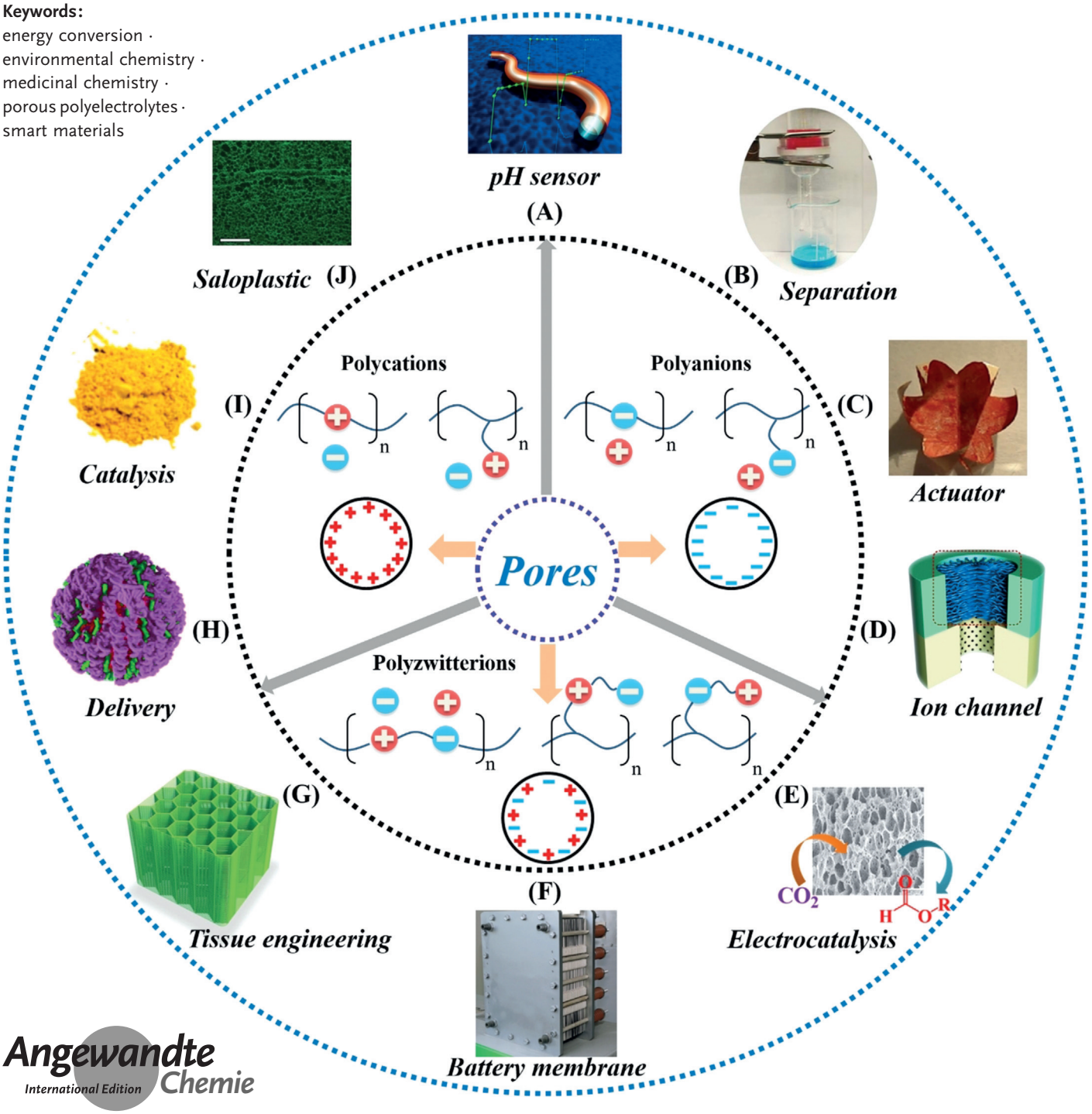

The past decade has witnessed rapid advances in porous polyelectrolytes and there is tremendous interest in their synthesis as well as their applications in environmental, energy, biomedicine, and catalysis technologies. Research on porous polyelectrolytes is motivated by the flexible choice of functional organic groups and processing technologies as well as the synergy of the charge and pores spanning length scales from individual polyelectrolyte backbones to their nano-/microsuperstructures. This Review surveys recent progress in porous polyelectrolytes including membranes, particles, scaffolds, and high surface area powders/resins as well as their derivatives. The focus is the interplay between surface chemistry, Columbic interaction, and pore confinement that defines new chemistry and physics in such materials for applications in energy conversion, molecular separation, water purification, sensing/actuation, catalysis, tissue engineering, and nanomedicine.

From the Contents

1. Introduction

Porous polymers have been actively pursued to address today's challenges in areas such as energy technology, sustainable development, clean water, and healthy living.[1] They are an essential part of modern industry and daily life, for example, in soft sponges, fabrics, and filters/separators that supply clean water and/or improve battery power.[2] Aside from amplified surface areas, porous polymers are characterized by high processability, cheap resources, light weight, and versatile chemistry for modification and functionalization.[1b] The boundaries of porous polymers are continuously widening, and their distinct forms include monolithic foams, powders, bulky resins, thin coatings, fibers, particles.[1,3] Structural features such as pore connectivity, accessibility, stability, and charge are crucial to their performance. Recent research has focused particularly on the synergy between Columbic charge and porous structures, especially when the pores are below 100 nm in size. At this extreme size end, electrostatic interaction is superimposed on nanoconfinement, so the mass transport is doubly controlled by the size and charge, which can have an impact on many processes, including ion exchange, molecular separation/gating, sensing, actuation, catalysis, energy conversion, and nanomedicine. The effect of ionic units in porous polymers has underpinned an emerging class of functional polymers—the porous polyelectrolytes.

Polyelectrolytes are polymers with ionized or ionizable groups in their repeating monomeric units.[4] They can be categorized as cationic, anionic, or zwitterionic polyelectrolytes (Figure 1, inner ring). Despite the large potential of porous polyelectrolytes (commonly used chemical structures are listed in the Supporting Information), their preparation remains a daunting task because conventional routes for neutral porous polymers fail or produce samples of low quality. For example, nonsolvent-induced phase separation (NIPS) and thermal-induced phase separation (TIPS) methods are the two standard methods for preparing porous filtration membranes.[5] Polymerization-induced phase separation was recently introduced to create hierarchical porosities in polymers.[6] However, these methods are difficult to apply to the vast majority of hydrophilic polyelectrolytes. To this end, methods such as layer-by-layer (LbL) assembly, nonsolvent complexation, and freeze-drying were developed to prepare porous polyelectrolytes with controlled pore architectures and enhanced surface areas for environmental, energy, and biomedical applications (Figure 1, outer ring). For example, combining the Donnan effect and pore-size sieving in porous polyelectrolyte membranes improved the separation/transport of ions, charged nanoparticles, and/or macromolecules. The incorporation of ions into porous conductive skeletons can improve the electron/hole mobility and promote electrochemical performances in batteries.[7] Last but not the least, nanoporous polyelectrolyte particles/micelles show a high load capacity for gene therapies in combination

[*] Dr. W. Y. Zhang, Prof. Q. Zhao
Key Laboratory of Material Chemistry for Energy Conversion and Storage, Ministry of Education
School of Chemistry and Chemical Engineering
Huazhong University of Science and Technology
Wuhan 430074 (China)
E-mail: zhaoq@hust.edu.cn
Dr. W. Y. Zhang, Prof. J. Y. Yuan
Department of Chemistry & Biomolecular Science
Center for Advanced Materials Processing
Clarkson University, Potsdam, NY 13699-5814 (USA)
Prof. J. Y. Yuan
Department of Materials and Environmental Chemistry (MMK)
Stockholm University, 10691 Stockholm (Sweden)
E-mail: jiayin.yuan@mmk.su.se

Supporting information and the ORCID identification number for one of the authors of this article can be found under: https://doi.org/10.1002/anie.201710272.

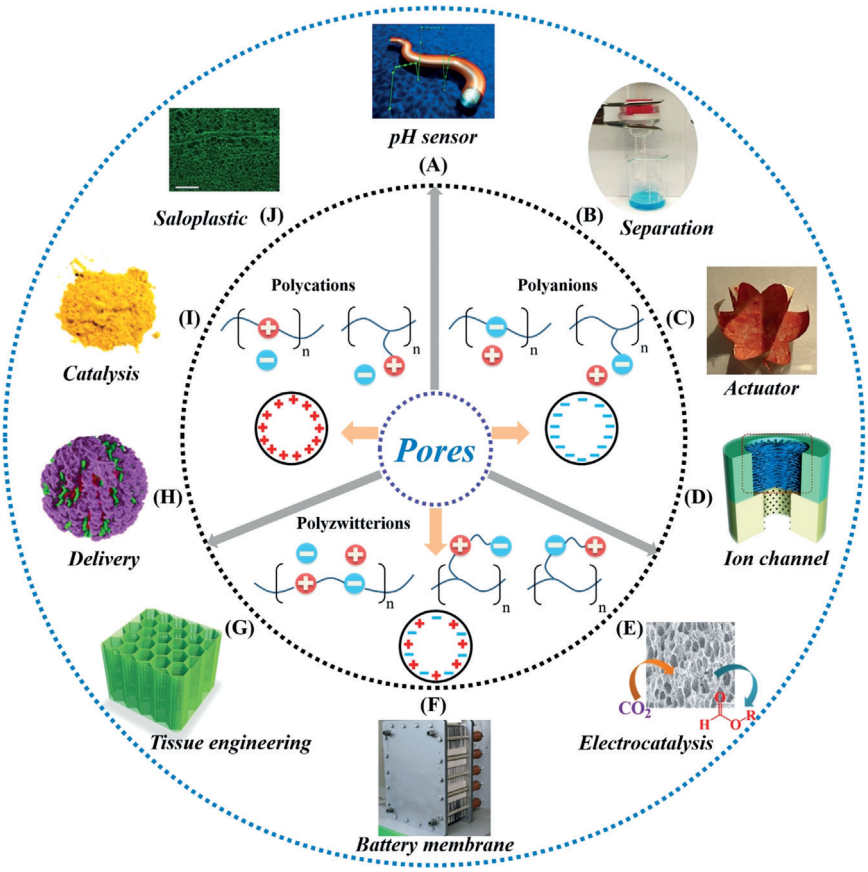

Figure 1. Classification of polyelectrolytes (polycations, polyanions, and polyzwitterions) and their corresponding applications: A) pH sensor;[45a] B) separation;[69f] C) actuator;[45b] D) ion channel;[88h] E) electrocatalysis;[84c] F) battery membrane;[85a] G) tissue engineering;[54] H) delivery;[94b] I) catalysis;[45g] J) saloplastic.[63e] The shapes of the ions are only a conceptual illustration and do not represent the physical size of each cation/anion. Reproduced from Refs. [45a,b,g, 54, 63e, 69f, 84c, 85a, 88h, 94b] with permission.

with programmed releasing as a result of delicately controlled particle–drug interactions at the charged pore interfaces.[8]

This Review deals with the preparation and applications of porous polyelectrolytes and their hybrids, in which polyelectrolytes sit at interfaces of pore channels. Functional materials derived from porous polyelectrolytes are also included. The Review starts with a brief introduction of porous polyelectrolytes, followed by methods to prepare their membranes, scaffolds, particles, and high surface area powders. Next, applications of porous polyelectrolytes in environmental protection, actuators, sensors, catalysis, energy conversion, nanomedicine, and biomedical scaffolds are detailed. Porous networks with charges, such as covalent organic frameworks (COFs) and metal-organic frameworks (MOFs), are not in the scope of this Review, since charged COFs/MOFs carry intrinsic micropores, while porous polyelectrolytes are mostly endowed with meso-/macropores and result in different confinement effects. In addition, porous polyelectrolytes can be processed more easily because of their polymer nature, and hence are more attractive for practical usage. Although there are various comprehensive reviews on porous polymers or porous materials,[9] porous polyelectrolytes have not yet been reviewed.

2. Porous Polyelectrolyte Membranes

Commercial porous polymer membranes, and in particular neutral polymers, account for an annually growing market of 8 billion USD. Their distinctive functions have led to a recent surge in the use of porous polyelectrolyte membranes (PPMs) in ion conducting/gating,[10] controlled delivery,[11] smart materials/interfaces,[12] nanodevices,[13] and biointerfaces,[14] but have suffered from limited synthetic methods. Most PPMs are prepared by LbL assembly, block copolymer (BCP) self-assembly, template strategies, and confined electrostatic complexation methods, as discussed in the following subsections.

2.1. Layer-by-Layer Porous Polyelectrolyte Membranes

LbL assembly is a thin film fabrication process whereby building blocks with complementary interactions are depos-

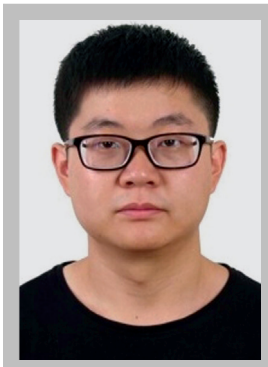

Weiyi Zhang obtained his master degree in 2014 from the Laboratory of Advanced Materials (LAM), Fudan university, China under the supervision of Prof. G. Zhou. He completed his PhD in 2017 at the Max Planck Institute of Colloids and Interfaces under the supervision of Prof. J. Yuan and Prof. M. Antonietti. He is currently carrying out postdoctoral research at Clarkson University, NY, US. His research focuses on functional polymeric materials.

Qiang Zhao graduated from the Department of Polymer Science and Engineering, Zhejiang University, China under the supervision of Prof. J. W. Qian. He carried out postdoctoral research at Zhejiang University (with Prof. C. J. Gao), the Max Planck Institute of Colloids and Interfaces (with Prof. J. Yuan and Prof. M. Antonietti), and the University of California Santa Barbara (with Prof. J. H. Waite). In 2017 he received the 1000 Young Talent grant from the Chinese government and started his independent research at the School of Chemistry and Chemical Engineering, Huazhong University of Science and Technology, China.

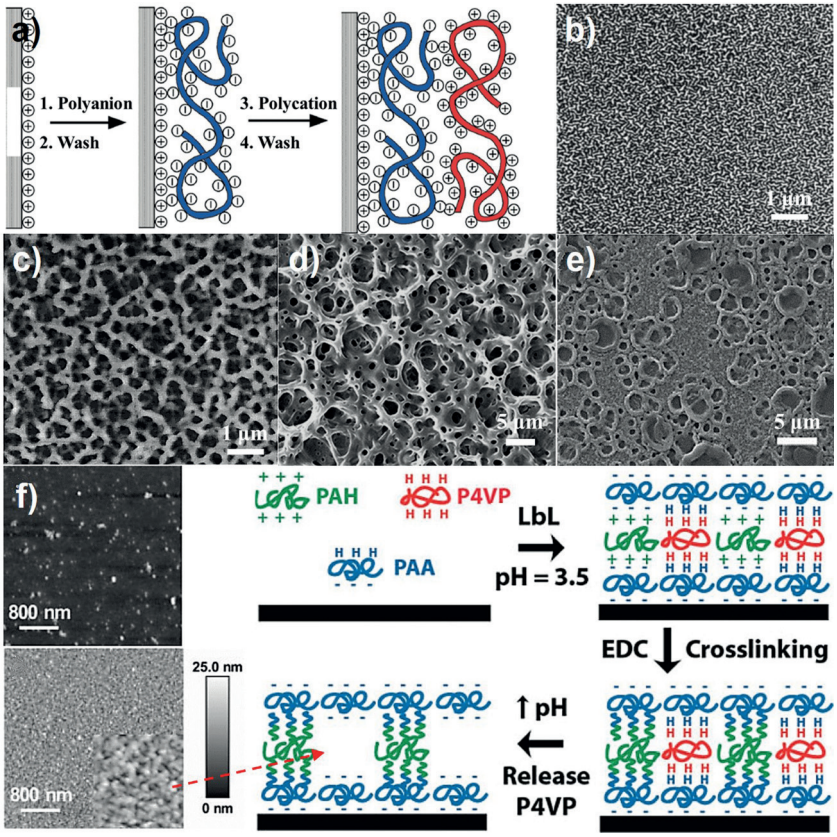

Figure 2. a) Schematic layer by layer assembly of oppositely charged polyelectrolytes.[15] b, c) Surface morphologies of a 21-layer PAA/PAH polyelectrolyte multilayer film ((PAA/PAH)$_{21}$) before (b) and after (c) immersion into a bath at pH 2.50.[18] d) Top-view SEM images of a (PAA/PAH)$_{20}$ film after immersion in an aqueous solution at pH 2.7 for 30 min without subsequent immersion in deionized water.[24] e) SEM images of PAH$_{8.5}$/PAA$_{3.5}$ films with 12.5 bilayers.[25c] f) Schematic illustration of the preparation and AFM images (before and after cross-linking) of PAH/PAA porous polyelectrolyte LbL membranes.[23] Reproduced from Refs. [15, 18, 23, 24, 25c] with permission.

ited onto substrates through alternating sorption.[15] This is a simple, practically powerful technique (Figure 2a) for producing films of precise thickness on a nanometers scale.[16] Most polyelectrolyte LbL films are dense and well-suited for molecular separation and as barrier films.[17] By modulating post-treatments and assembly conditions, LbL films can be made porous for applications such as sensors, smart coatings, and controlled delivery vehicles.

2.1.1. *Post-Treatment Methods for Porous LbL Films*

Rubner and co-workers reported porous polyelectrolyte LbL films made from poly(acrylic acid) (PAA) and poly(allylamine hydrochloride) (PAH; Figure 2b,c).[10,18,19] Three-dimensionally (3D) interconnected porous PAA/PAH multilayer films with pore sizes ranging from 100 to 500 nm were obtained by tuning the pH value of the assembly solutions. The subsequent exposure of these films to neutral water resulted in discrete open pores with diameters of 50 to 200 nm, which could be chemically fixed by annealing above 200 °C. Inspired by the work of Rubner and co-workers, the use of other stimuli such as salts,[20] electric field,[21] and light[22] was investigated. These studies showed it was possible to create tunable pores with diameters ranging from tens of nanometers[23] to micrometers (Figure 2d).[24] By using the same NaCl concentration in both the assembly and washing steps, Caruso and co-workers proved that smooth films were obtained first and exposure to water resulted in their evolution into porous films with regular, discrete, nanometer-sized pores.[20a] These authors also discovered that the film morphology depended on the film thickness, which is indicative of a dewetting mechanism for pore formation.

This model of pore formation was further exploited to engineer porous LbL films. Lee and co-workers prepared PAA/PAH polyelectrolyte multilayer films with tunable surface properties and hierarchical pores by using high-molecular-weight PAH and PAA.[25] Zacharia and co-workers created pores by exposing poly(ethylene imine)/PAA films to an electric field.[21] Zhang and co-workers fabricated a light-sensitive porous film, and created pores 10–100 nm in size by degradation of poly-L-lysine (PLL) and DNA terminated with 5-(4-aminophenyl)-10,15,20-triphenylporphyrin (APP) groups by irradiation with light.[22] This work enables the remote control of porous structures with tunable pore densities and pore sizes. Zhang et al. proposed a two-step mechanism for the formation of pores in PAA/poly(4-vinylpyridine) (P4VP) multilayer films in a basic solution.[26] This proposal consisted of the quick dissolution (e.g. ca. 1 min) of PAA at pH 12.5 and the gradual reconformation of P4VP polymer chains remaining on the substrate. The same group also studied the effects of electrostatic interactions[27] and the substrate[28] on pore formation.

Jiayin Yuan studied chemistry at Shanghai Jiao Tong University (China) in 1998. He received his MSc from Universität Siegen (Germany) in 2004 and PhD from Universität Bayreuth (Germany) in 2009 with Prof. A. H. E. Müller. He joined the Max Planck Institute of Colloids and Interfaces in Potsdam first as a postdoctoral researcher and from 2011 as a research group leader. He received an ERC Starting Grant in 2014, Dr. Hermann-Schnell Award in 2015, and the Dozentenpreis from the Fund of Chemical Industry in 2016, and a Wallenberg Academy Fellowship from the Kunt and Alice Wallenberg Foundation in 2017. He completed his Habilitation in 2015, and after a position at Clarkson University (USA, 2017), he is now an Associate Professor at Stockholm University (Sweden).

2.1.2. Templated Porous LbL Films

An alternative to post-treatment is the preparation of LbL PPMs by a templating strategy.[23,29] Caruso and co-workers described the assembly of PAH and P4VP with PAA at pH 3.5 (Figure 2 f).[23] The film was first thermally cross-linked to fix the PAH/PAA pair, and subsequently the P4VP component was erased at pH 10 by disrupting the hydrogen bonding between the P4VP and PAA to yield nanoscale pores (10–50 nm). Zhuo et al. circumvented the cross-linking reaction by introducing a disulfide-bearing polycation template that is cleavable under reductive conditions, such as phosphate-buffered saline.[33] The polycation template was mixed with PAH and assembled with poly(sodium 4-styrenesulfonate) (PSS), which formed porous multilayer films on reductive removal of the template. Recently the same group constructed porphyrin-containing porous LbL films through photodegradation of component polyelectrolytes (PLL and DNA). Importantly, both the number and sizes of the pores were controlled by the illumination time, thus offering a new route to porous LbL films.[22]

2.1.3. Porous LbL Films Based on Unconventional Building Blocks

Building blocks other than conventional polyelectrolytes, for example, zwitterionic polyelectrolytes (Figure 1, inner ring), polyelectrolyte complex (PEC) particles, pillar[5]arenes/cucurbit[8]uril derivatives, and graphene,[30] have recently been utilized to prepare nanoporous LbL membranes. A zwitterionic polyelectrolyte carries both a cation and anion in the same monomer unit, and tends to form intramolecular associations through ionic interactions.[28b] An and co-workers reported the zwitterionic polyelectrolyte poly(4-vinylpyridiniomethane carboxylate) which, after blending with poly(dimethyldiallylammonium chloride) (PDADMAC), assembled in an LbL fashion with PAA.[20b] The ionic interaction between poly(4-vinylpyridiniomethane carboxylate) and PAA was interrupted in a 0.15 M NaCl solution and resulted in nanoporous PDADMAC/PAA membranes. The zwitterionic polyelectrolyte can even be removed under physiological conditions as a result of its weak bonding with the anionic polymers.[29] Sun and co-workers used salt-containing nonstoichiometric PAA-PAH PEC particles as building blocks,[31] and stressed the important roles of the salts in the formation of the pores. This interpretation was supported by other studies, whereby LbL membranes made from PEC particles with little to no salts were found to be dense.[32]

Ogoshi et al. presented a rare example of an LbL film assembled from two oppositely charged pillar[5]arene derivatives (Figure 3 a).[34] The active pores were the inherent cavity of the pillar[5]arene molecules (ca. 5 Å), and could be precisely controlled at the Ångstrom level. The microporous pillar[5]arene LbL membrane could take up *para*-dinitrobenzene (ca. 4.3 Å) and reject *ortho*-dinitrobenzene and *meta*-dinitrobenzene (both ca. 5.9 Å). In addition to size selection, surface charges on this LbL film determined its ability to adsorb guest molecules, similar to nanofiltration and reverse osmosis membranes that are governed by a combination of

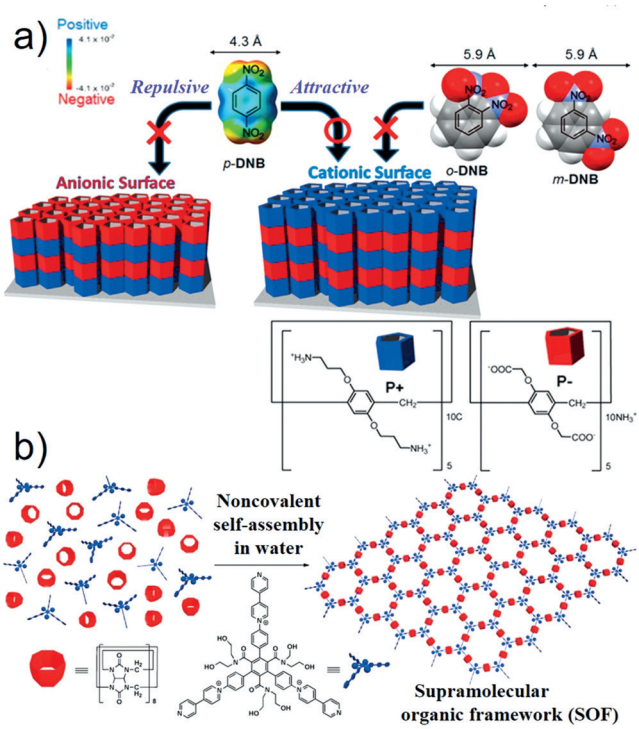

Figure 3. a) Size-selective and surface-potential-dependent molecular recognition of a microporous LbL film ("P+": pillar[5]arene-NH_3^+; "P−": pillar[5]arene-COO^-).[34] b) Self-assembly of different building blocks with cucurbit[8]uril in water.[35c] Reproduced from Refs. [34, 35c] with permission.

size and charge effects. Li and co-workers produced a 2D supramolecular film by complexation of the preorganized triangular aromatic guests containing 4,4′-bipyridin-1-ium with cucurbit[8]uril.[35c] Self-assembly at a 2:3 molar ratio in water led to single-layered periodic honeycomb-shaped 2D films with a pore diameter of 3.70 nm (Figure 3 b). Feng and co-workers furthered extended this method to prepare 1.8 nm thick monolayers with areas up to 0.25 cm^2.[35d] The ability to modulate pore sizes and film thicknesses at the Ångstrom/nanometer level is crucial for molecular separation, particularly for fairly similar molecular sizes, for example, xylene isomers. Moreover, it renders the host–guest recognition chemistry viable in the solid state,[35] in contrast to the vast majority of previous solution-based studies.

2.2. Block Copolymer (BCP) Porous Polyelectrolyte Membranes

BCP PPMs are accessible by breath-figure, self-assembly, and templating methods. The breath-figure method is based on the use of amphiphilic copolymers to stabilize water droplets that are condensed in a water-immiscible organic solvent.[36] Karthaus and co-workers found that negatively charged polyion complexes could reduce the surface tension of the condensed water droplets and stabilize their two-dimensional arrangements, thus enabling the formation of well-defined honeycomb membranes.[37b] BCP self-assembly is known to give rise to a wealth of ordered polymer

microstructures,[38] which can be used to engineer PPMs if one of the BCP blocks is a polyelectrolyte. As such, a variety of BCPs consisting of a neutral hydrophobic polystyrene (PS) block and an ionic hydrophilic block (e.g. PAA[37] and P4VP[39]) were investigated. Ma and co-workers reported that the hydrophilicity of the PAA block was essential to form porous PS-*b*-PAA films with better regularities and larger pores.[40] The degree of ionization of PAA was found to determine the time for the transformation of the wettability behavior of the PS-*b*-PAA honeycomb membrane and its water contact angle.[37c] Stenzel and co-workers exploited PS-*b*-PAA honeycomb membranes as a scaffold for cell growth, whereby the PAA block was designed to dope polypyrrole for better performance of the cell cultures.[37a] Smaller pores were found to enhance cell attachment, which indicates that Columbic charge has an impact on the structure, formation kinetics, and physicochemical properties of the membranes.

Peinemann et al. combined BCP self-assembly with the NIPS process for the one-step preparation of nanoporous BCP membranes without a template (Figure 4 a).[41] The PS-*b*-P4VP BCP was dissolved in a mixture of dimethylformamide (DMF) and THF. The polymer solution was cast onto a glass plate, dried at room temperature for 10 s, immersed in water for 24 h, and eventually dried under ambient conditions. Interestingly, the cross-section of the porous structure was similar to that of a normal NIPS-based macroporous membrane, while the well-defined nanopores on the top surface originated from the BCP self-assembly. This method has the advantage of combining the two distinct porous morphologies in a one-step scalable process. The same group later further expanded this process, including by combination of the spray or dip coating technique with NIPS (Figure 4 b).[41f]

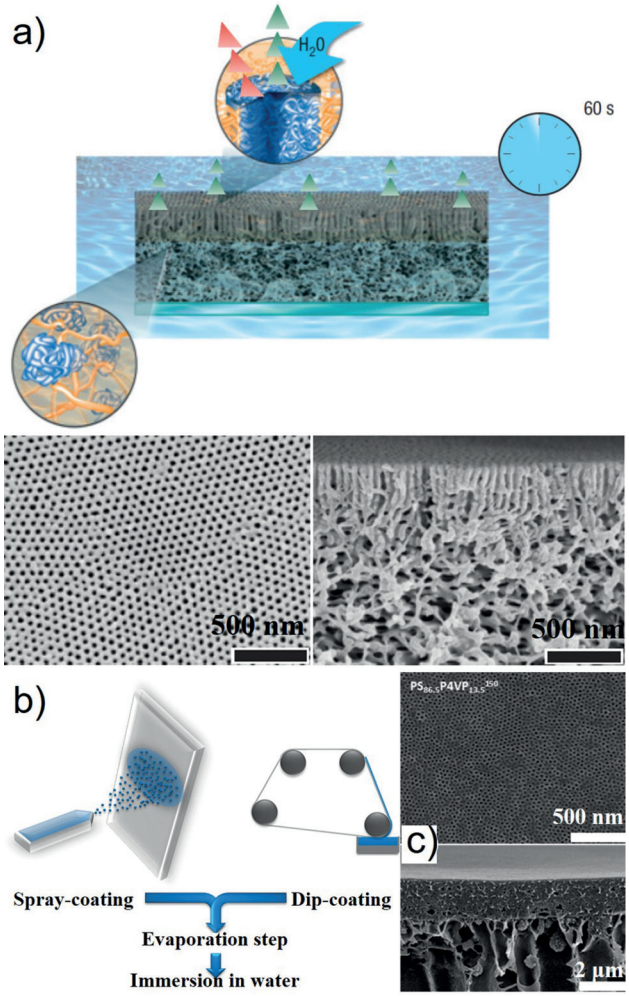

Figure 4. a) Formation of an asymmetric membrane from PS-*b*-P4VP BCP. Immersing a PS-*b*-P4VP film in a water bath leads to a NIPS and the formation of a porous sublayer; simultaneously the P4VP-lined cylinders grow in length. The green and red arrows represent the evaporation of THF and DMF, respectively. SEM images of the surface (bottom left) and cross-sectional (bottom right) structures of a PS-*b*-P4VP nanoporous membrane.[41e] b) Membrane production by either spray or dip coating. c) SEM images of the top and cross-section of self-assembled membranes made from PS-*b*-P4VP with different molecular weights and P4VP contents.[41f] Reproduced from Refs. [41e,f] with permission.

2.3. Polyionic Liquid (PIL) Porous Membranes

PILs are polyelectrolytes synthesized by the polymerization of ionic liquid (IL) monomers. The IL species confer PILs with unique physiochemical properties, such as solubility in some organic solvents that were previously considered as nonsolvents for conventional hydrophilic polyelectrolytes, glass transition temperatures down to −50 °C, high surface activities, and inflammability. Dense PIL membranes have been exploited by Gin and Noble for the capture/separation of CO_2[42] and ion conduction.[43] The hydrophobicity of some PILs is a distinctive feature that renders their porous PIL membranes stable in water. Three major strategies—counter-anion exchange,[44] confined electrostatic complexation,[45] and hard template[46]—have recently been used to fabricate porous PIL membranes.

The effect of the counteranion on PIL porous structures was pioneered by the Texter group (Figure 5).[44] A transparent and compact gel was produced by the copolymerization of methyl methacrylate in a microemulsion with a surfactant-like bromide-containing IL monomer in the presence of a dimethacrylate cross-linker. When bromide (small and hydrophilic) was exchanged by a bulky PF_6^- anion, the PIL gel became semitransparent and contained internal interconnected macropores.[44a] This poration process was reversible by shuttling between water and dimethyl sulfoxide (DMSO) solvents, and is a generic phenomenon of similar copolymers developed by the same group.[44b] The phase diagram of this poration system was later studied in detail,[44b,c] and the mechanism was extended to film systems.[47a] Yan et al. prepared a PIL porous membrane with high uptake of metal ions, whereby the porous morphology could be tuned by ab-/desorption of metal ions.[44e] Recently, Gao and co-workers prepared a series of cross-linked porous PIL networks by replacing the bulk anion (salicylate) with a halide ion. The as-prepared PILs exhibited nanoparticle morphologies and hierarchical pores with a specific surface area of up to 200 $m^2 g^{-1}$ that featured good catalytic activity in the cycloaddition reactions of CO_2 with epoxides.[47b]

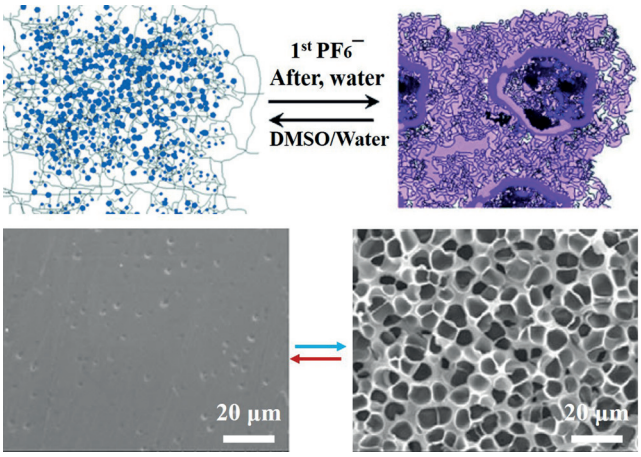

Figure 5. Spinodal decomposition of a cross-linked bicontinuous gel to form an open-cell porous material upon exposure to a poor solvent. Bottom: SEM pictures of the poly(1-(2-acryloyloxyundecyl)-3-methylimidazolium tetrafluoroborate) PIL after microemulsion polymerization (left) and after treatment with an aqueous 0.1 m KPF_6 solution (right).[44a] Reproduced from Ref. [44a] with permission.

The hard templating method has also been applied to prepare porous PIL membranes. IL monomers were bulk-polymerized in situ in face-centered cubic SiO_2 nanoparticle templates.[46b–e] The silica template was removed by etching with hydrofluoric acid, thereby resulting in 3D ordered macroporous PIL membranes. The as-prepared membranes highlight the precise control over the pore shapes and sizes, and function well as photonic crystal sensors. However, the removal of silica templates is labor-intensive and evolves hazardous etching reagents.

To circumvent the hard templating method, electrostatic complexation was exploited to fabricate hierarchically structured (nano)porous PIL membranes with an unusual gradient in the complexation degree along their cross-sections (Figure 6).[45a] In a typical experiment, a cationic hydrophobic PIL and PAA were dissolved in DMSO. The PAA stays neutral in DMSO and is, thus, homogeneously mixed with the PIL in solution without complexation/precipitation. The mixture solution was cast as a thin liquid film on a glass plate, dried at 80 °C, and finally immersed in an aqueous ammonia solution. The ammonia and water molecules then diffused into the film to deprotonate the PAA and so introduce electrostatic complexation between the PIL and PAA, whereas the PIL was simultaneously phase-separated from the water to create pores (Figure 6a). The first generation of membranes prepared by this method feature hierarchical porous systems along the cross-section, namely, a macroporous skin and a bulk 3D interconnected nanoporous layer, bearing pores from 30 to 100 nm (Figure 6b).

The second generation aims to improve the membrane performance by controlling the charge density, the molecular weight of acids, and the additives. Such membranes have either a homogeneous porous cross-section or a gradient distribution of pore sizes. For example, membranes with pores ranging from 80 nm to 2.5 μm were tailored by choosing benzoic acid derivatives (Figure 6c);[45e] membranes impregnated with cellulose nanofibrils showed a tensile strength of up to about 10.4 MPa, which is much higher than commercial porous polymer filtration membranes;[45f] membranes bearing

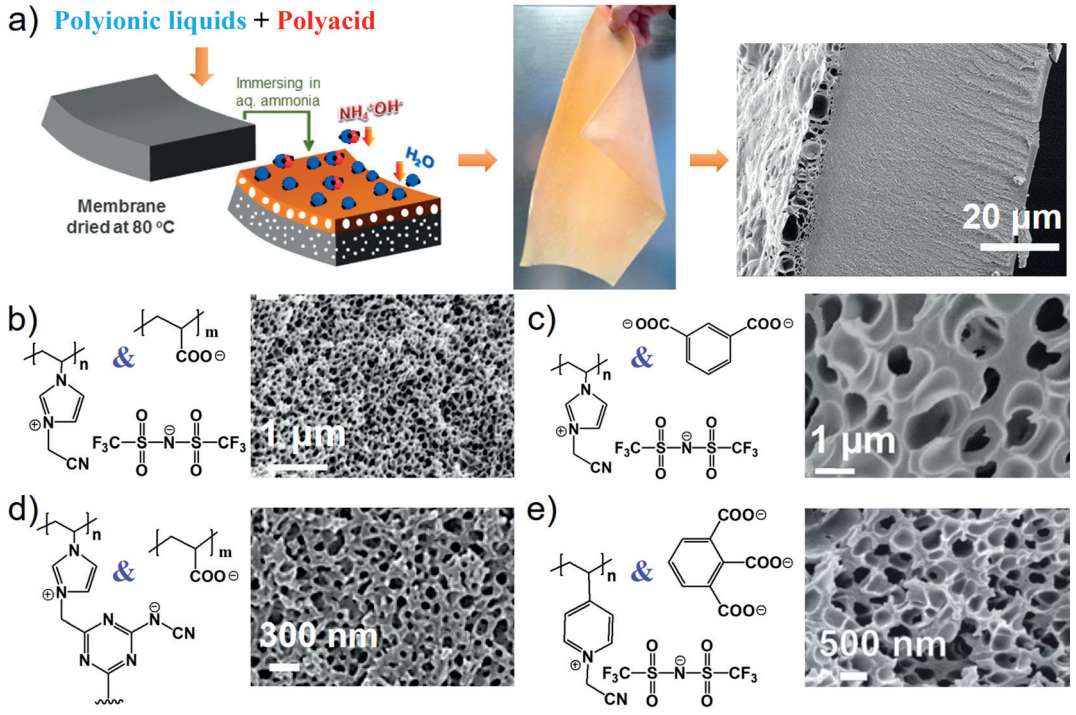

Figure 6. a) Preparation of a nanoporous polyelectrolyte membrane made from a mixed solution of a cationic PIL and PAA in DMF.[45a] b–e) Chemical compositions and SEM images of a porous PIL membrane with different chemical compositions.[45d–f] Reproduced from Refs. [45a,d–f] with permission.

dicyanamide anions were thermally cross-linked by a 1,3,5-triazine network (Figure 6d) to enhance their stability in an ionic environment, which makes these membranes useful as separators for lithium ion batteries.[48] This method was further broadened to other polyelectrolytes, such as polyvinylpyridinium compounds (Figure 6e)[45d] and other hydrophilic polyelectrolytes.[49a] It was even applicable to mussel-inspired polyelectrolyte complexation triggered by solvent exchange to yield a robust wet adhesive with porous structures depending on the catechol content in the polyelectrolyte system.[49b]

In parallel, the groups of Vancso and Xu exploited the electrostatic complexation method to engineer redox-responsive porous PIL membranes[50] and porous anion-exchange membranes,[51] respectively. The pore structures were found to be switchable between more-open and more-closed states depending on the electrochemical redox potential. This feature was attributed to the redox-responsive ferrocenylsilane moieties in the membrane. Such a membrane was applied as a flow-rate controller that could be used for gated filtration, catalysis, and controlled release.[50] Zheng and co-workers used this method to synthesize a cationic PIL carrying azobenzene side groups. The pores were responsive toward irradiation with ultraviolet light, and could selectively adsorb cationic dyes.[51e] Instead of PAA, Zhang and co-workers used a poly(acrylic acid-*co*-acrylonitrile) copolymer to prepare a porous nanofiltration membrane with improved mechanical strength for filtrations under external pressure.[52]

3. Porous Polyelectrolyte Scaffolds

3.1. Freeze-Dried Porous PEC Scaffolds

Freeze-drying of an aqueous polyelectrolyte solution is a straightforward method for preparing macroporous polyelectrolytes with micrometer-scale pores. It has been widely used to prepare scaffolds for tissue engineering,[53] which requires stable porosity in an aqueous environment to provide adequate spaces and channels for cell migration and the efficient transport of nutrients and metabolic wastes. In addition, biocompatibility, degradability, and mechanical strength are necessities that must be considered for polyelectrolyte scaffolds. In this regard, the polycation chitosan has been complexed with various polyanions such as pectin, polygalacturonic acid, sodium alginate, carboxymethyl cellulose, and silk fibroin.

To prepare PEC scaffolds, the polyelectrolyte components were mixed to obtain either a solution or precipitate, followed by freeze-drying and modulation. The structures of such PEC scaffolds depend on both the chemical nature of the starting polyelectrolytes and the processing parameters. Ding and co-workers used a facile assembly process followed by freeze-drying and ionic cross-linking to prepare a hydrogel scaffold. The obtained 3D elastic bulk nanofibrous structures based on alginate featured shape-memory behavior, elastic-responsive conductivity, and could be injected (Figure 7a,c).[54] Zhang and co-workers reported that the viscosity of the chitosan/sodium alginate solution had an impact on the pore structures

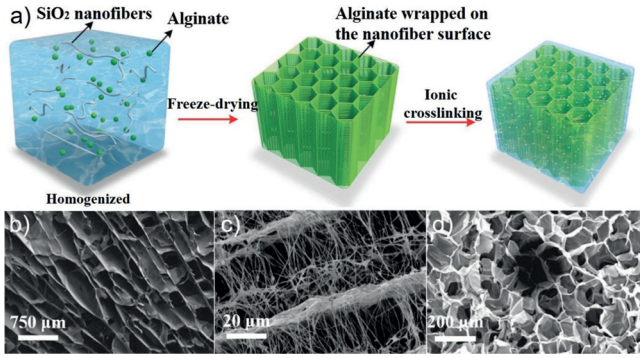

Figure 7. a) Freeze-drying for the preparation of porous scaffolds. b–d) Representative SEM images of PEC scaffolds generated by the freeze-drying method.[54,55,60a]. Reproduced from Refs. [54, 55, 60a] with permission.

and mechanical properties of the scaffold, and excessive acetic acid in the system caused degradation of the pores (Figure 7b).[55]

Zhang and co-workers have focused on the preparation, structure regulation, and application of chitosan/sodium alginate porous scaffolds.[56] A chitosan/sodium alginate blend solution was introduced into 24-well cell-culture plates, freeze dried, and cross-linked with $CaCl_2$. The electrostatic complexation between chitosan and sodium alginate enhanced the scaffold strength, thereby giving rise to a compressive modulus of 8.16 MPa and a yield strength of 0.46 MPa at a porosity of 92%.[56b] Moreover, the chitosan/sodium alginate PEC scaffold has a high degree of tissue compatibility that promotes the proliferation of bone-forming osteoblasts, thus providing a promising scaffold material for clinical trials. Polygalacturonic acid and chitosan were exploited by Katti and co-workers to prepare fibrous PEC scaffolds featuring highly porous structures that arose from the coalescence of PEC particles at the interface of ice crystals.[57] The same group later incorporated hydroxyapatite particles into the scaffolds to enhance the adhesion and proliferation of osteoblast cells.[57a]

Wu et al. developed a three-component (chitosan, polyglutamate, and carboxymethylcellulose) porous PEC gel for application as an injectable scaffold.[58] Enhanced bone regeneration was achieved, and the early stage healing of bones was accelerated by adding $CaSO_4 \cdot 2H_2O$ to the scaffold. Chen and Fan found that the internal porosity of the carboxymethylcellulose/chitosan porous scaffolds was increased through the incorporation of the cellulose component.[59] The adhesion, spreading, cell capacity, and 3D configurations of pulp cells were improved in the PEC scaffolds compared to the pristine chitosan scaffolds.

Silk fibroin, despite its brittleness, is one of the most attractive biopolymers for the tissue engineering of bones, cartilage, and ligaments. Several groups have explored chitosan/silk fibroin scaffolds as a consequence of the ionic complexation between the two polyelectrolytes.[60] Feng and co-workers found that optimized chitosan/silk fibroin scaffolds promoted the proliferation of the human hepatoma cell line significantly (Figure 7d).[60a] Bhardwaj and Kundu

reported that both the mechanical performance and antibacterial properties were improved by the electrostatic complexation between silk fibroin and chitosan.[60c] Coimbra et al. prepared chitosan/pectin PEC precipitates by mixing the two aqueous solutions at pH 4.5.[61] Freeze-drying at −20 °C led to macroporous PEC scaffolds, on which human osteoblast cells could proliferate with noncytotoxic degradation by-products.[62] The same group also prepared chitosan/sodium hyaluronate porous PEC scaffolds with smaller pores for tissue engineering.[61]

3.2. Saloplastic Porous PECs

Recently, Schlenoff and co-workers coined the concept of "saloplastic" PECs, which are ionically cross-linked materials that can be reshaped by breaking sufficient cross-links using concentrated salt solutions.[63] Interestingly, these materials can also feature porosity and can be easily processed through treatment with various salts. This endows the saloplastic PECs with unique mechanical properties that are suited for bioimplants. Saloplastic PECs have been reviewed by the same authors in Ref. [64].

4. Porous Polyelectrolyte Particles

Porous particles with appropriate particle sizes, colloidal stability, loading capacity, releasing properties, and biocompatibility are sought after for nanomedicine. Porous polyelectrolyte particles can undergo multiple and modulated interactions with targeted charged biomacromolecules (e.g. DNA, protein) to afford an increased payload such as with polyion-DNA complexes for gene therapy.[8b] Templated LbL assembly[65] and BCP self-assembly[66] are emerging methods for preparing porous polyelectrolyte particles.

Caruso and co-workers prepared porous particles for in vivo delivery and therapy by the infiltration of polyelectrolytes into mesoporous silica templates followed by cross-linking and template removal. The size of the polyelectrolyte coil in the dipping solutions must match the channel size (ca. 30 nm) of the mesoporous template to facilitate polymer infiltration into the template particles. The authors utilized low-molecular-weight PAA ($MW = 2000\ g\,mol^{-1}$) in a dipping solution containing 0.7 M NaCl to force infiltration of the polymer under sonication. After each assembly cycle, the adsorbed polymers were cross-linked by heating the dried sample at 160 °C for 2 h. Eventually the silica templates were removed with hydrofluoric acid to yield porous polyelectrolyte particles with pore sizes of around 5–50 nm.[65g] This work opened up a generic pathway to nanoporous polyelectrolyte particles with tailored compositions, such as nanoporous protein (lysozyme, cytochrome *c*, and catalase) particles,[65e] peptide particles,[65d] and drug-loading particles.[65c,d,f] The controlled delivery of drug payloads was modulated through cleavage of sensitive bonds such as disulfide[65f] and hydrazine (Figure 8a)[65c] bonds between the model drugs and the polyelectrolytes.

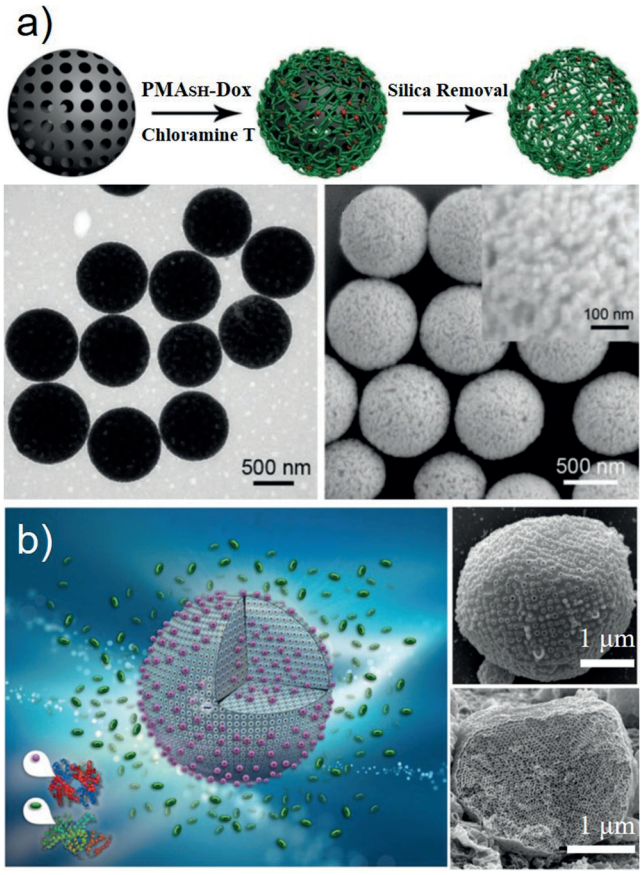

Figure 8. a) The modular assembly of silica-templated drug-loaded polymer particles and pH-dependent drug release after endocytosis in a cancer cell.[65c] b) Selective separation of bovine serum albumin (green ellipsoid) and bovine haemoglobin (magenta sphere) using the PS-*b*-PAA particle at pH 5.8. The figures on the right-hand side are SEM images of particles with regular nanometer-sized pores of high density.[66] Reproduced from Refs. [65c, 66] with permission.

Yan et al. exploited a templating method to prepare nanoporous polyelectrolyte/nanoparticle composites.[65h,i] Inorganic nanoparticles (e.g. citrate-Au and γ-Fe_2O_3) were loaded into porous calcium carbonate microparticles in the first step. The PLL polyelectrolytes were then infiltrated into the template and cross-linking was carried out with glutaraldehyde. Finally, the particle template was removed to yield porous colloidal polyelectrolyte/nanoparticle spheres. The template-assisted assembly highlights the controlled loading density of nanoparticles and flexible variation of polyelectrolytes on demand, thus allowing the fabrication of 3D hybrid colloidal spheres with multiple functions in a simple and controllable manner.

Nanoporous polymer particles with gated pores and high protein sorption capacity were prepared by Peinemann and co-workers using PS-*b*-PAA BCP (Figure 8b).[66] The copolymer was first dissolved in a toluene/methanol mixture, whereby the toluene and methanol are good solvents for the PS and PAA blocks, respectively. Spherical particles with dense (2.1×10^{13} pores m^{-2}) and uniform pores (ca. 27 nm) perpendicular to the surface were obtained after adding a fivefold excess of methanol to the BCP solution. The phase

diagram and kinetics of the self-assembled structures revealed that the self-assembly mainly occurs in three steps: 1) vesicles and lamella, 2) Schoen gyroid, 3) Schwarz P structure. These particles were negatively charged at all the pH values tested (3–10), which indicates that the surface is rich in the PAA block. As such, the particles could separate bovine serum albumin and immunoglobulin A proteins, which have similar sizes (6.8 nm versus 14 nm) but different isoelectric points (4.7 versus 7.3), because the surface charges gate the pore entrance through electrostatic interactions with the charged proteins.

5. High Surface Area Porous Polyionic Liquids

The porous polyelectrolytes discussed above were mostly macroporous with low specific surface areas ($< 100\ m^2 g^{-1}$) or mesoporous in a thin-film state. The remarkable chemical and physical properties of PILs has led to rapid progress in high surface area bulk polyelectrolytes. Three methods have been exploited so far, including templating,[46a,67] nonsolvent complexation,[35b,68] and hyper-cross-linking.[69]

5.1. Template Method

By employing rather small commercial silica nanoparticles, LUDOX TM 50 (ca. 25 nm), as templates, Wilke et al. prepared mesoporous PILs with well-defined mesopore sizes and shapes as well as high specific surface areas up to $200\ m^2 g^{-1}$.[46a] The interstitial voids of an opal-like mesoporous silica template were first filled up with a liquid IL monomer/initiator mixture. Mesoporous PILs were then obtained by polymerization of the IL monomers at 200 °C and subsequent removal of the silica templates. Wang and co-workers invented a soft template route towards hierarchical meso-/macroporous PIL monoliths with tunable pore structures.[67a] The IL monomer 1-allyl-3-vinylimidazolium chloride was self-polymerized in an aqueous solution containing the copolymer P123 ($EO_{20}PO_{70}EO_{20}$) as a soft template. Removal of the template by ethanol extraction afforded the targeted porous monolith. Odriozola and co-workers utilized ILs as porogenic solvents to prepare nanoporous PILs.[67b] The method is facile, scalable, and generic, but the porous PILs only have moderate specific surface areas up to $90\ m^2 g^{-1}$.

5.2. Nonsolvent Complexation Method

In contrast to covalent cross-linking, which is frequently exploited to obtain polymers with high surface areas, ionic cross-linking in conventional polyelectrolytes is less popular because the dynamic nature of the electrostatic complexation in water makes it hard to freeze the conformation of the polyelectrolyte chain and to stabilize the pore structures. This limitation has been circumvented by using hydrophobic PILs, as exemplified by mesoporous PIL complexes.[35b,68] In a typical formulation, a hydrophobic PIL was blended with PAA in DMF or DMSO solvent (the dissolving solvent), which was added to a solution of ammonia in ethanol (the complexation solvent) to yield porous powders with specific surface areas and pore volumes of up to $300\ m^2 g^{-1}$ and $1\ mL g^{-1}$, respectively. Notably, high surface areas were obtained only when the complexation solvent was a poor solvent for both polymers. For example, dense materials were obtained in water which could dissolve PAA. On this basis, the authors hypothesized that the collapsed polymer chains in their nonsolvents were instantaneously fixed by ionic cross-linking, which resulted in frozen porosity. The nonsolvent complexation strategy applies to various PILs[68c,d] and acid molecules including multivalent acids[68b] and pillar[5]arene supramolecular acids.[35b] It is conceptually simple, straightforward, and applies to a fairly large family of PILs with exceptional performance and stability in organic media. However, there is less control over the pore size of the products and they are susceptible to aqueous media with high ionic strength, thus necessitating covalent cross-linking for stabilization of the structure and applications in water.

5.3. Hyper-Cross-Linking Method

The hyper-cross-linking method has been exploited to prepare a series of porous PIL composites.[69a–d] The solvothermal copolymerization of divinylbenzene (DVB) and vinylimidazolium IL monomers was use by Kuzmicz et al. to prepare mesoporous PIL monoliths with a highest surface area of $935\ m^2 g^{-1}$.[69a] The prepared PILs contained an abundance of embedded mesopores and adjustable IL functionalities, thereby offering two distinct applications in N-heterocyclic carbene catalysis and as porous carbon precursors. The method is simple and can even be conducted when there are space limitations. For example, performing the method in the interstices within cellulose fiber-based tissue paper led to the generation of a mesoporous PIL/tissue paper hybrid membrane.[69f] Zhang et al. used a solid-state C–O cross-coupling reaction to prepare charged porous polymers. This mechanochemical strategy is "green", facile, and the resulting porous polymers show good activity and stability for SO_2 capture.[70]

Xiao and co-workers prepared nanoporous PIL/PDVB copolymers by post-modification.[69e] Firstly, DVB was copolymerized with 1-vinylimidazole under solvothermal conditions to yield superhydrophobic mesoporous copolymers with a water contact angle of approximately 150°. Quaternary alkylation led to the neutral imidazole groups being converted into positively charged imidazolium units, which drop the water contact angle to $< 10°$. A similar strategy was adopted by Bordiga and co-workers, who proposed a two-step route to PILs with specific surface areas up to $800\ m^2 g^{-1}$.[69b] The authors used a Debus–Radziszewski click reaction to prepare hierarchically porous PILs with a specific surface area of $400\ m^2 g^{-1}$. These materials exhibited good performance in CO_2 sorption (CO_2 uptake: $2\ mmol g^{-1}$ of at 1 bar and 273 K) through the formation of an imidazolium carboxylate zwitterion.[71] Hyper-cross-linking has so far produced porous polyelectrolytes with the highest surface areas at the expense of a low ionic charge density in the material.

Engineering high surface area polyelectrolytes ($>1000\ m^2\ g^{-1}$) with high charge density remains a challenge.

6. Applications

Porous polyelectrolytes are endowed with enriched functionalities because of the synergy between the pores and charge at multiple length scales. For example, PPMs show advanced implications for the separation/sensing/transport of ions, charged nanoparticles, and/or macromolecules, which is attributed to the combination of the Donnan effect and size exclusion. Moreover, the amplified particle–drug interactions at the charged pore interfaces has led to porous polyelectrolytes showing a high load combined with a programmed release for gene therapies. Interestingly, polyelectrolytes with porous structures exhibit superior performance in organic catalysis both as the catalysts and/or support materials.

6.1. Environmental Applications

6.1.1. Environmental Remediation

Common heavy metal ions in waste water, such as copper, lead, nickel, and zinc, are hazardous pollutants that threaten human health. Porous polyelectrolytes are effective for their removal because of the ion–polyelectrolyte interactions. Zhang and co-workers grafted PAA chains onto a porous poly(glycidyl methacrylate) monolith, and the resulting system showed a Cu^{2+} adsorption capacity as high as $35.30\ mg\ g^{-1}$ as a result of favorable complexation with the numerous carboxylate groups in the monolith.[72] Chen and co-workers prepared negatively charged porous polyacrylonitrile polymers with improved adsorption capacities for Hg^{2+}, Ag^{+}, and Cu^{2+}.[73] Encouraging results were also obtained with porous sodium alginate, which exhibited a high adsorption capacity of $90.0\ mg\ g^{-1}$ for Cr^{III} ions.[74] In addition to aqueous adsorption, porous PILs show improved performance in the removal of pollutants from organic solvents[35b,68b] and the adsorption of CO_2.[46a,68d,71] Ammonia is a highly toxic industrial gas that is hazardous to both health and the environment. Brønsted acidic porous polymers showed a high uptake of ammonia gas ($2\ mmol\ g^{-1}$ at 0.05 mbar equilibrium pressure) as a result of proton transfer between the ammonia molecules and the acidic groups combined with strong hydrogen-bonding interactions.[75]

Besides their application as adsorbents, porous polyelectrolytes with responsive pore sizes can also function as separation membranes.[76] Gu and Wiesner tuned the pore size (23–48 nm) and molecular weight cutoff (MWCO) of nanoporous PS-*b*-P4VP membranes by modulating the amount of glycerol additives in the casting solutions.[77] This approach provided a route to nanoporous membranes with tunable applications for both ultrafiltration and nanofiltration without compromising the mechanical properties of the membrane.[78] Stamm and co-workers demonstrated the multifunctionality of nanoporous polyelectrolyte membranes in catalysis and pH-switchable filtration, whereby the pores arose from the random stacking of PS-*b*-P4VP particles.[79] The membrane rejected 97% lysozyme protein and the permeation of water was pH-dependent. Minko and co-workers have also investigated a series of responsive PPMs.[76a,80] For example, the permeability of a sodium alginate porous membrane towards rhodamine B dye molecules was near zero at pH 7, consistent with the closed pore state at this pH value.

Very recently, Im and co-workers proposed an initiated chemical vapor deposition method to prepare cross-linked, conformal polyelectrolyte coatings.[81] By using these methods the authors deposited polyelectrolyte coatings on stainless-steel mesh to fabricate a hydrophilic and underwater oleophobic membrane, which exhibited a high separation efficiency (>99%) and unprecedentedly high permeation flux ($2.32\times10^5\ L\ m^{-2}\ h^{-1}$) in oil/water separations. This approach is a generic method to prepare porous polyelectrolyte hybrids with broadly tuned surface chemistry, hydrophilicity, and functional groups. The groups of Xu and Wang engineered hierarchical porous anion-exchange membranes with improved ion-exchange capacity and selectivity, which show good performance in the recovery of acid from waste water by means of diffusion dialysis.[51] Fouling of filtration membranes is an important issue that degrades the separation performance with increasing operation time. Several reports show that incorporating zwitterionic polyelectrolytes into porous polymer membranes improved their antifouling properties.[82]

6.1.2. Environmental Sensing and Actuation

Polyelectrolyte chains carrying functional organic units are known for their responsiveness towards environmental stimuli (moisture, light, temperature, pH, etc.). These properties could be engineered into sensors and actuators. For example, Qian and co-workers found that the sensing speed of a nanoporous PDADMAC/PAA LbL film coated on an optical fiber with a thin core was one order of magnitude faster than dense PDADMAC/PAA coatings, because the pore channels speed up the molecular diffusion when switching between different pH values.[20b] This edge property brought by the ion-responsiveness of the polyelectrolytes and fast transport in porous channels was further evidenced with porous PIL pH sensors,[45a] which featured an even faster sensing speed because of the higher density of pores compared with the porous LbL films. Vancso and co-workers introduced polyferrocenylsilane (PFS) moieties into porous polyelectrolyte membranes and prepared redox-responsive devices. The reversible switching of the pore structures was dependent on the redox state of the ferrocene unit in the polymer backbone (Figure 9d).[83a]

As for soft actuators, pore structures in PIL membranes were found to improve actuation speed and sensitivity. Zhao et al. used a PILTf_2N/C-pillar[5]arene complex membrane to fabricate a porous polyelectrolyte actuator (Figure 9a–c).[45b] A gradient in the degree of electrostatic complexation along the membrane cross-section was accompanied by heterogeneous swelling, thus bending the membrane in contact with the organic vapors. Meanwhile, pores were proven to accelerate the diffusion of the solvent gas stimulus to the site of action. As a result of this synergy, the actuation speed toward

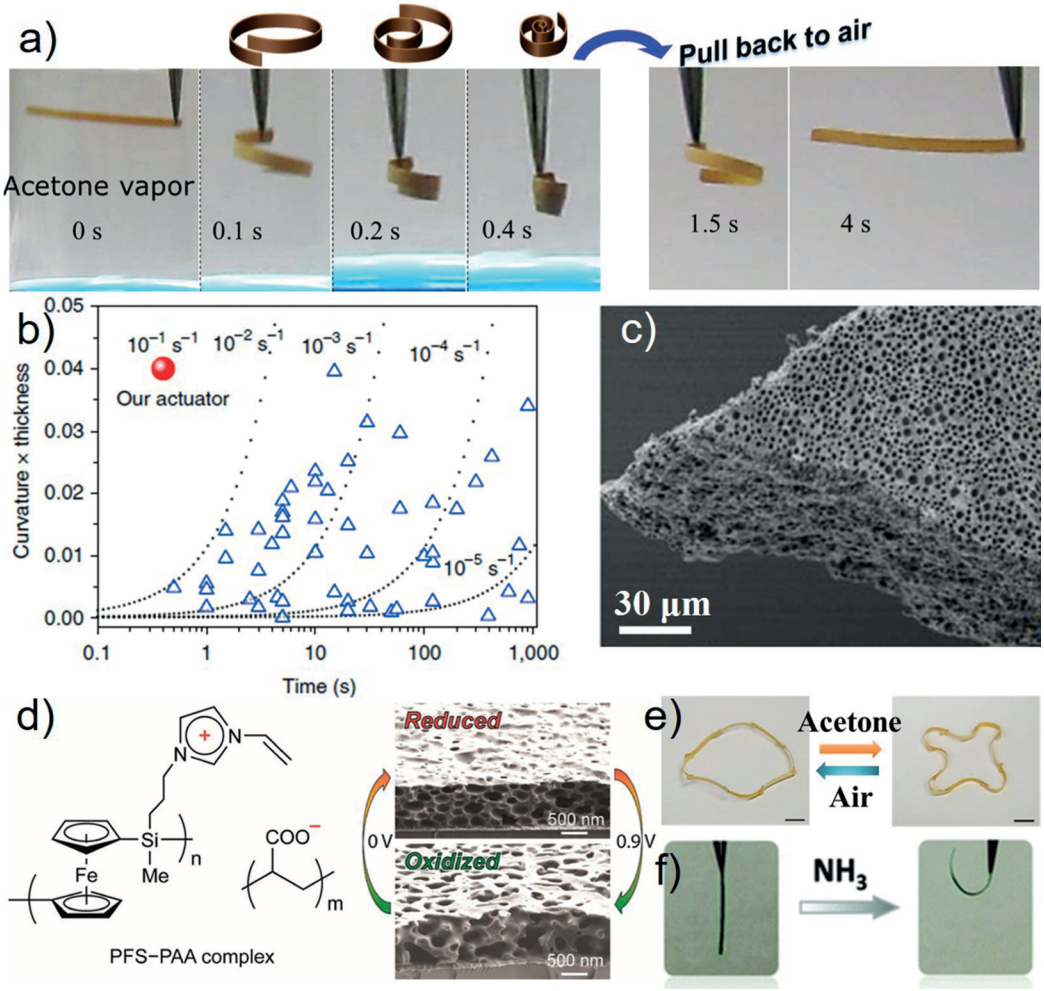

Figure 9. a) Adaptive movement of a PILTf$_2$N/C-pillar[5]arene complex membrane (1 mm × 20 mm × 30 mm) in acetone vapor (24 kPa, 20 °C, left) and then back in air (right). b) Comparision of the actuation rate to literature results. c) SEM image of the porous membrane actuator.[45b] d) Chemical structures of a polyferrocenylsilane-based redox-responsive porous polyelectrolyte membrane and SEM images of its more-closed and more-opened states when reduced and oxidized, respectively.[83a] e) Actuating and recovering of PIL-modified tissue paper membranes. The SEM image is a cross-sectional view of the membrane.[83b] f) Adaptive movement of a hybrid membrane formed from PIL and a metal-organic framework (11 mm × 2 mm × 38 µm) in NH_3 gas.[83c] Reproduced from Ref. [45b, 83a–c] with permission.

acetone vapor (24 kPa, 20 °C) is at least one order of magnitude faster than other synthetic polymer actuators. Porous PIL actuators were capable of distinguishing 13 types of solvents as well as sensing acetone molecules at as low as 0.1 mol % in water.[45c] Furthermore, Lin and co-workers introduced a PIL-modified tissue paper to improve the actuator flexibility (Figure 9e).[83b] Last but not least, the porous PIL actuator system is compatible with other materials chemistry, such as hybridization and crystallization of metal-organic frameworks, thus resulting in higher mechanical strength or responsiveness towards NH_3 gas (Figure 9f).[83c]

6.2. Energy Applications

6.2.1. Electrocatalysis/Batteries

PILs are known to be precursors of nitrogen-doped carbon materials. Recently, porous PILTf$_2$N-PAA membranes were pyrolyzed under vacuum to template the formation of nitrogen-doped porous carbon membranes.[84] The synthetic route has so far been scaled up to 10.5 × 3.5 cm^2. These carbon membranes featured a high graphitic order, hierarchical pore structures, and nitrogen doping that are favorable for electrochemical applications. For example, after functionalization with cobalt nanoparticles,[84a] Co/CoP Janus-like nanoparticles,[84b] or carbon nanotubes,[84c] these hybrid membranes turned out to be active non-noble metal electrocatalysts toward overall water splitting, the hydrogen evolution reaction, or CO_2 reduction reaction (Faradaic efficiency of 81 % for the production of formate).

Porous polyelectrolyte membranes were also applied directly in flow batteries as ion separators. The groups of Li and Zhang conducted the LbL assembly of polyelectrolytes on both the inner pore wall and the surface of sulfonated poly(ether ether ketone)/poly(ether sulfone) membranes (Figure 10).[85a] This resulted in the membrane surface being conferred with hydrophilicity and high ion conductivity, while

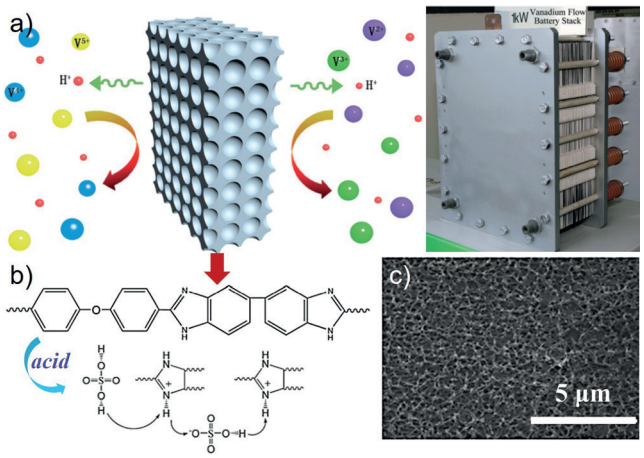

Figure 10. a) Schematic and real view of a cell stack prototype of the sponge-like porous polybenzimidazole membrane utilized in vanadium flow batteries. b) Chemical structure and proton conducting mechanism of a porous polybenzimidazole membrane. c) SEM image of the cross-section of the membrane.[85a] Reproduced from Ref. [85a] with permission.

the polyelectrolytes on the pore walls reduced the pore size of the substrate for higher ion selectivity. Similar porous polyelectrolyte membranes based on poly(ether sulfone)/sufonated poly(ether ether ketone) blends[85b] and cross-linked networks on the pore walls of polysulfone[85c] were also realized and applied in vanadium flow batteries. Enhanced proton conducitivity, stability, and ion selectivity were achieved. The responsive porous polyelectrolyte membranes function as efficient separators for vanadium flow batteries over a wide range of current densities. Very recently, the groups of Xu and Guiver reported a microporous polyelectrolyte membrane based on Trögers base that exhibited good chemical stability and a hydroxide conductivity of 164.4 mS cm under optimal operating conditions. The membrane was easily synthesized from two commercial monomers and the high conductivity was thought to be related to the synergy of the intrinsic microporosity and the positive charge, which is appealing for fuel cells, flow batteries, and dialysis applications.[86]

6.2.2. *Ion Gating and Ion Pumps*

Biological membranes are excellent at controlling mass transport through ion and water channels in an energy-efficient way. Translating this gating capability into synthetic materials is a compelling topic that is in its infancy. Responsive polyelectrolytes, when anchored to nanoscale channel surfaces, can play an enabling role in gating water permeability and ion transport. One way to mimic biological gating properties is with the self-assembled BCP isoporous membranes. Peinemann and co-workers studied the pH-responsive gating behavior of an isoporous PS-*b*-P4VP membrane prepared by NISP in combination with the BCP self-assembly approach.[41b] The water flux increased more than two orders of magnitude upon changing the pH value from 2 to 8, and is reversible. While the dependence of the porous morphology and water flux on the pH value stems from the pH-dependent protonation/deprotonation properties of the P4VP block, the strong response to pH is ascribed to the unusually high porosity coupled with a uniform distribution of pore sizes. In parallel, Azzaroni and co-workers used single conical nanopore channel gating devices prepared by the LbL technique.[87] The surface charge on the pore walls decreased rapidly as the number of PAH/PSS layers increased. The ion-transport properties of the modified channel were studied in detail, which laid the chemical foundations for the LbL modification of nanochannels and the physical principles of ion transport across nanopores functionalized with the supramolecular assemblies. Other polyelectrolytes have also been investigated for ionic gating.[88] Ali et al. found that significant differences exist between the carboxylate and phosphonate groups with respect to calcium binding and transportation.[89b] Soler-Illia et al. reported that a strong polyelectrolyte (poly[(2-(methacryloyloxy)ethyl)trimethylammonium chloride) could be grafted inside mesoporous membranes by thermal- or light-initiated free-radical polymerization, with the polyelectrolyte grafting content or macroscopic positioning under fine control.[89a] Significant efforts have also been directed to ion channels by combining responsive polyelectrolytes with task-specific substrates bearing channels of distinctive geometry. Jiang and co-workers designed nanochannels with various geometries, sizes, and gate positions by integrating responsive polyelectrolytes (e.g. PAA, P4VP, and DNA) to surfaces of pore walls to explore smart ion gates.[88] An hour-glass-shaped nanochannel with two wide open bases (250–300 nm) and a narrow center (10–30 nm) was made, and PAA was grafted only onto one side of the channel by plasma-induced radical grafting (Figure 11 a).[88b] The PAA-modified, asymmetric "smart" channel shows a reversible and reproducible open/closed switching state upon alternating the pH value of the test solutions between 2 and 10. Ion-gating devices that were multiresponsive to temperature and pH were built by grafting poly(*N*-isopropylacrylamide) onto the other side of the nanochannel.[88c]

The ability of a single system to show multiresponsive behavior brought these nanochannel devices closer toward real-life applications, for example, ion pumps. A cooperative pH-responsive double-gate nanochannel was designed that was asymmetrically functionalized with two weak polyelectrolytes, PAA and P4VP, respectively, at the two ends of the channel (Figure 11 b).[88e] As such, this bioinspired single ion pump is able to mimic three key features of biological ion pumps, namely, transformation of the ion pump into an ion channel under an asymmetric pH stimuli, an alternating ion pumping process under symmetric pH stimuli, and a fail-safe ion pumping feature under both symmetric and asymmetric pH stimuli. Ion channels and ion pumps have been used for energy conversion including electricity generation and voltage response on a laboratory scale, which indicates their promising future in real-life applications.

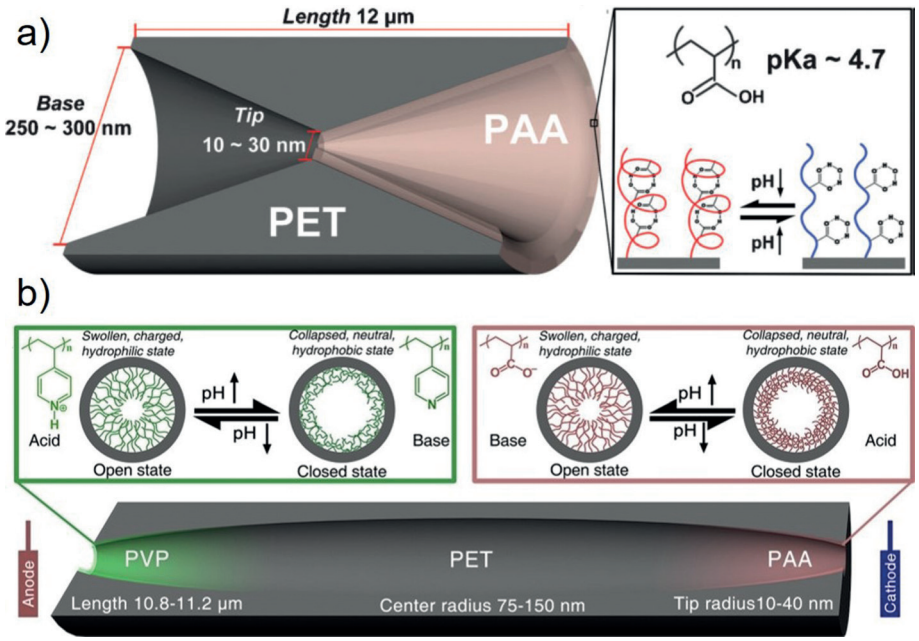

Figure 11. Schematic representation of cross-sections of a) a single hour-glass-shaped nanochannel with one side grafted with PAA;[88b] b) an artificial cooperative pH-responsive double-gate nanochannel with an acid-driven PVP gate and a base-driven PAA gate immobilized on the inner surface of the left and right sides of the tip, respectively. The inset shows the gating mechanisms for both ends of the ion channels.[88e] Reproduced from Refs. [88b,e] with permission.

6.3. Biomedical Applications

6.3.1. Tissue Engineering

Porous 3D polyelectrolyte scaffolds and films have been exploited for tissue engineering, tissue repair, and drug delivery. The Zhang group, along with others, pioneered porous chitosan scaffolds for cell culture,[56a,90] gene tissue engineering (Figure 12d),[56b,91] gene delivery (Figure 12b),[92] etc. They found that porous chitosan/sodium alginate scaffolds could mimic the growth environment of glioma cells in vitro by providing a microenvironment that is similar to that encountered in xenograft tumors in vivo.[56a] The same group grew cells from glioblastoma cell lines on porous 3D chitosan/sodium alginate scaffolds to promote the proliferation and enrichment of cells that possessed the hallmarks of cancer stem cells.[90] In another study on the repair of bone defects, a porous chitosan/sodium alginate scaffold promoted the growth of mesenchymal stem cells with a spherical morphology instead of monolayers (Figure 12a).[91b] Scaffolds made exclusively from chitosan were also investigated.[91c,d] The PEC scaffold composed of chitosan, γ-polyglutamic acid, and carboxymethylcellulose was used to treat dental bone defects (Figure 12c).[58b,91d] The crystallinity of the chitosan scaffold was found to correlate positively with the chitosan concentration and inversely to the solution acidity.[91d] A 3D chitosan scaffold was developed with a pore size, pore orientation, and mechanical stiffness favorable for the regeneration of skeletal muscle tissue.[91c] The scaffolds with an appropriate Young's modulus were able to produce myotubes with sizes comparable to the diameter of native innervated muscle fiber. Chen et al. reported that chitosan/hyaluronic acid scaffolds assisted the proliferation of fibroblasts and expression of EGF, VEGF, and IGF-1 genes.[93]

6.3.2. Nanomedicines

Porous polyelectrolyte particles have been exploited for in vivo circulation (Figure 13c),[65a] cell internalization, and drug delivery.[65a,b,94] Caruso and co-workers prepared porous disulfide-bonded poly(methacrylic acid) (PMA) particles which rapidly traffic from early endosomes to lysosomes within a few minutes following internalization.[65a]

The intracellular mobility was dependent on the particle size, shape, surface chemistry, and cell physiology. For example, the association of phagocytic blood cell with porous poly(ethylene glycol) (PEG) particles was

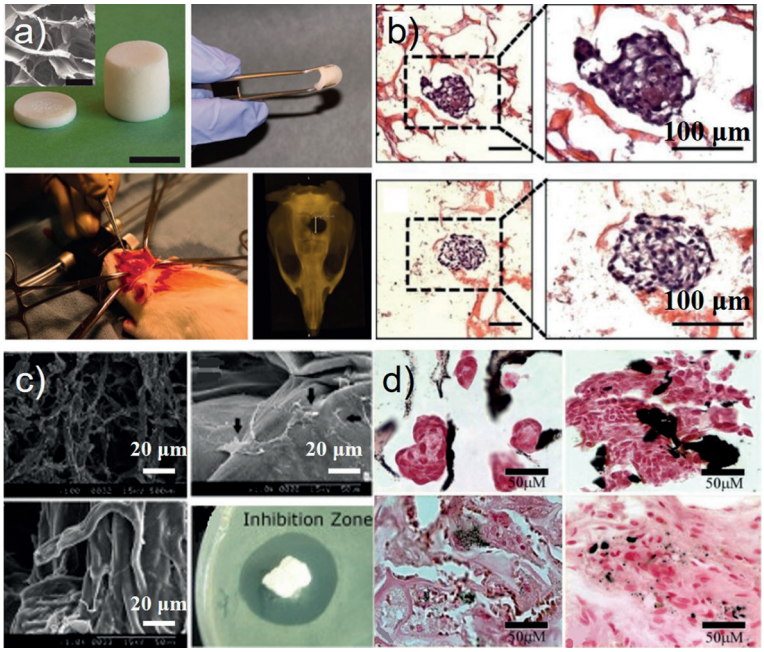

Figure 12. Applications of polyelectrolyte scaffolds. a) Use of chitosan/alginate scaffolds for the repair of cranial defects.[91b] b) Hematoxylin and eosin staining of TRAMP-C2 tumor spheroids grown in chitosan/alginate scaffolds for 12 days.[92] c) Morphology and microstructure of a PEC scaffold and attached MC3T3E1 cells on a PEC scaffold after incubation.[58b] d) Optical images of the Von Kossa histological stain assay of chitosan/alginate scaffolds after culture in vitro and implantation in vivo.[56b] Reproduced from Refs. [56b, 58b, 91b, 92] with permission.

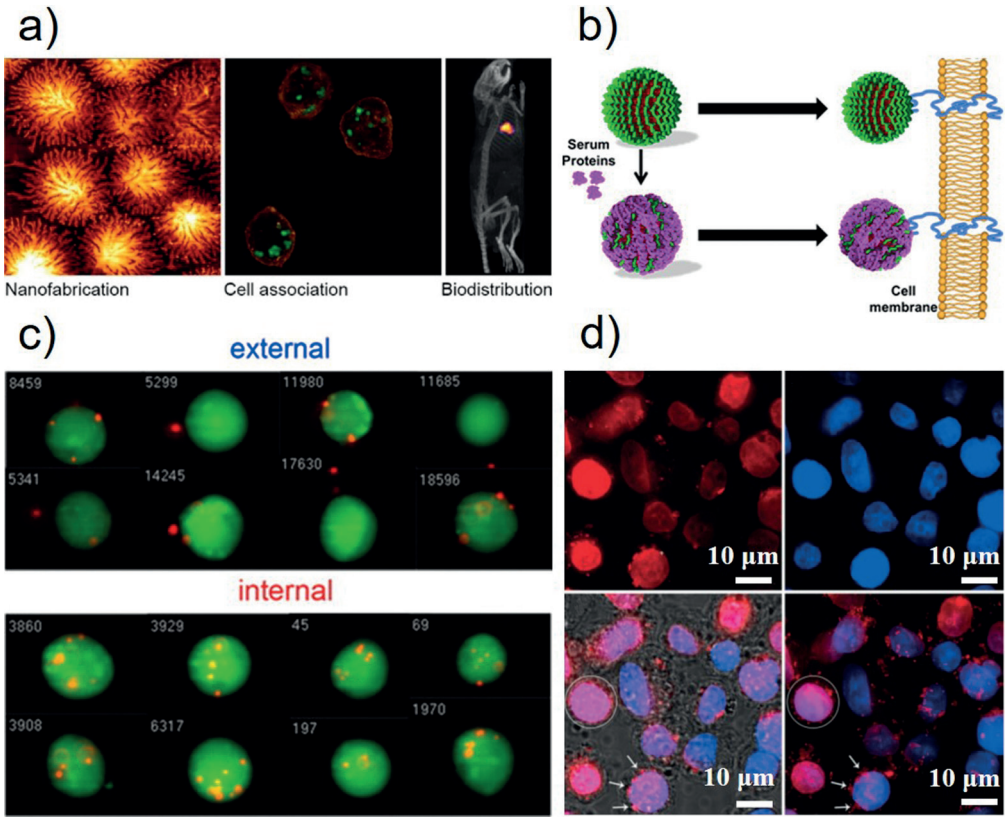

Figure 13. Applications of porous polyelectrolyte particles. a) Illustration of the nanofabrication, cell association, and biodistribution of PEG hydrogel particles.[94c] b) Targeting of cancer cells using capsules or particles with a "hard" protein corona formed on the surface of polymer particles functionalized with monoclonal antibodies.[94b] c) Representative images of labeled PMASH internalized (bottom) and external surface-bound particles (top) particles in HeLa cells by imaging flow cytometry.[65a] d) Representative deconvolution microscopy images of LIM1899 cells treated with PMASH-doxorubicin particles at a particle/cell ratio of 1000:1.[65c] Reproduced from Refs. [65a,c, 94b,c] with permission.

reduced upon decreasing the particle size from 1.4 μm to 150 nm. The retention of smaller PEG particles (150 nm) in blood 12 h after injection had increased fourfold compared with PEG particles larger than 400 nm (Figure 13a).[94c] With regard to cell targeting, functionalization of the porous PMA particles with humanized A33 monoclonal antibodies (huA33 mAb) enhanced the binding power of the particles to the cell membrane of LIM2405þ cells (Figure 13b).[94b] Redox modification of the protein surface of the porous particle affected both the physicochemical properties and the immunogenic performance.[94a] In recent studies, Caruso and co-workers were able to control the delivery of doxorubicin, an anticancer drug, by using pH-labile bonding between the drug and the porous polyelectrolyte particles (Figure 13d).[65c]

In addition to particles, porous polyelectrolyte films have also been exploited for drug delivery. Ji and co-workers found that the pore structures in a porous polyethylenimine/PAA multilayer film could self-heal upon exposure to saturated humidity.[95] These dynamic characteristics were used for encapsulation of the representative hydrophobic drug triclosan in the film for surface-mediated drug delivery. The porosity enabled a high drug loading in the film, and the subsequent sustained release stemmed from the humidity-dependent pore gating. This dynamic porous polyelectrolyte film acts as a robust platform for the delivery of various active species, for example, hydrophobic drugs, nanoparticles, or macromolecules, in a wide variety of biomedical applications.

6.4. Catalysis

The coulombic charges on polyelectrolytes render them well-suited nanoreactors for the preparation of metallic nanoparticles with high catalytic performance.[96] The charged nanoporous network could also improve the pore affinity, polarity, colloidal stability, and accessibility.[3b,97] For example, Ma and co-workers combined covalent organic frameworks (COFs) with a catalytically active polyelectrolyte by inner-channel polymerization of its monomer. The hybrid porous polyelectrolyte showed significantly improved catalytic efficiency in the cycloaddition of epoxides, as a result of the synergy between the flexibility of the polymer chain and ionic COF–polyelectrolyte interactions (Figure 14).[98] Moreover, Liu and co-workers discovered that porous polystyrene resins with an ultrahigh concentration of amino groups are effective in Friedel–Crafts alkylation and Beckmann rearrangement reactions. Aside from the properties of the ionic interfaces, the charges can stabilize ligands or metal ions and/or serve as the catalyst themselves under basic[99] or acidic[100] conditions. For example, Bruening and co-workers fabricated a porous

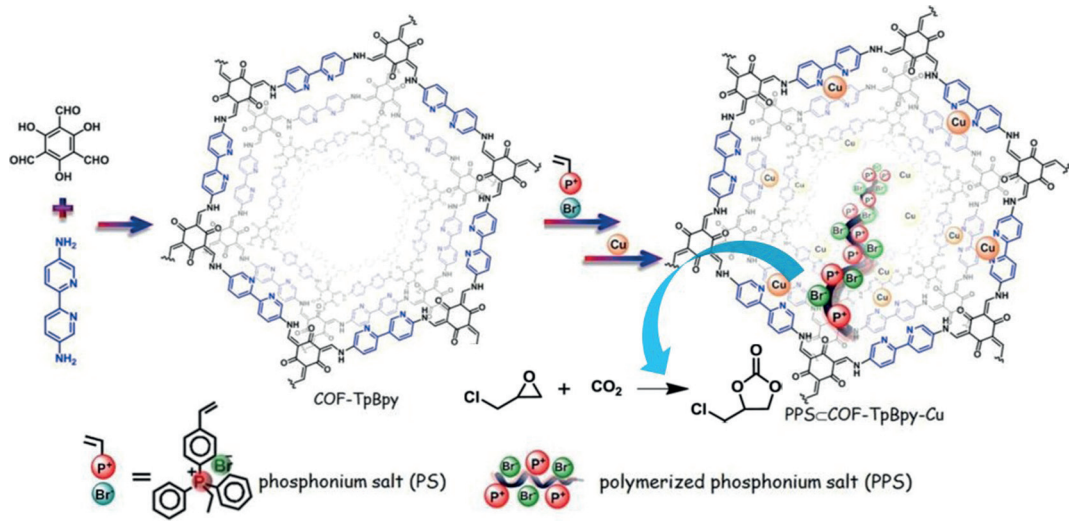

Figure 14. Synthesis of PPS⊂COF-TpBpy-Cu and structures of COF-TpBpy and PPS⊂COF-TpBpy-Cu, which were used as catalysts for the cycloaddition of epichlorohydrin; TpBpy = 1,3,5-triformylphloroglucinol and 5,5′-diamino-2,2′-bipyridine.[98] Reproduced from Ref. [98] with permission.

polyelectrolyte/anodic aluminum oxide/gold nanoparticle composite membrane for the catalytic reduction of 4-nitrophenol.[101] The high accessibility of the gold nanoparticles results in a highly efficient membrane-flow catalysis, whereby > 99 % of the 0.4 mM 4-nitrophenol was reduced at linear flow rates of 0.98 cm s^{-1}. Similar conditions can be found in hollow fiber membranes[102] and porous PIL membranes.[103]

Porous PILs have also shown special properties in catalysis and other applications.[67c] Zhao et al. prepared porous PIL complexes in which the porous network was first loaded with as high as 13 wt % copper ions and next used as a composite catalyst for the highly efficient aerobic oxidation of hydrocarbons under mild conditions.[68a] Zhou and co-workers synthesized a high surface area porous PIL network with high ion density and basicity for the cycloaddition of CO_2 and epoxides.[104] The groups of Wang,[69c] Xiao,[69e] and Bordiga[69b] copolymerized several IL monomers with divinylbenzene to prepare mesoporous PILs that function as a solid–liquid heterophase catalyst. Interestingly, these mesoporous PILs have good accessibility to organic compounds and resistance to CO_2/H_2O. The catalytic function of the porous PIL family was further expanded by loading with palladium nanoparticles or α-CuV_2O_6 nanobelts for the oxidation of benzyl alcohol[105] or the direct catalytic synthesis of 2,5-diformylfuran from fructose,[106] respectively.

7. Conclusion and Outlook

Porous polyelectrolytes show a fine synergy between ionic units and surface chemistry within confined pore environments engineered by polymer chemistry methods and/or polymer processing techniques. Appealing properties can be generated to serve a wide range of fields, including environmental remediation, liquid purification/separation, ion rectification, battery membranes, scaffolds, drug delivery, and catalysis. Conventional methods for the fabrication of porous neutral polymers apply only in part to porous polyelectrolytes because of their ionic character. Specific methods such as LbL assembly, freeze-drying, inter-polyelectrolyte complexation, etc. offer a simplified synthetic route and better control over the pores and structural motifs in the polyelectrolytes. They can provide access to honeycomb patterns and gradient elements, which enable a plethora of possibilities in materials design. In contrast to other ordered porous materials (COFs, MOFs, zeolites, etc.), porous polyelectrolytes are easily prepared in technologically more relevant forms such as membranes, thin films, fibers, and particles because of their polymeric nature. Nevertheless, control over the surface area and micropore size in porous polyelectrolytes is far below what is demanded. For example, a specific surface area of 1200 $m^2 g^{-1}$ is common in porous neutral polymers or frameworks, but has not yet been achieved in porous polyelectrolytes. There is indeed much room left for developing new synthetic concepts to modulate the pore size, pore shape, and surface functionality at multiple length scales, and the micropores in particular.

One of the most significant effects of porous polyelectrolytes is the electrostatic interactions in nanopores, which might enable new ion purification and separation techniques. Energy applications of porous polyelectrolytes are rapidly expanding, such as ion pumps and battery membranes. When applied as carbon precursors to produce electrode materials, the porous polyelectrolytes can, during carbonization, facilitate pore preservation, heteroatom doping, and impregnation of inorganic nanoparticles. Porous polyelectrolytes have been investigated for a long time in the biomedical area, where the ionic interaction plays a pivotal role in determining the microstructures of scaffolds and drug vehicles, and in controlling the drug-loading and -releasing properties. In terms of catalysis, porous polyelectrolytes can create an adaptive pore environment for individual reactions by tuning the nanoconfinement effect, the ionic interaction with substrate molecules, and the choice of surface groups. Porous polyelectrolytes with new structural platforms, for example, fibers or 2D porous polyelectrolytes, have been

much less explored and represent vast future opportunities. These examples have greatly advanced the research into the application of porous polymers and, in our opinion, will remain the main driving force in the future.

Porous polyelectrolytes make up an interdisciplinary research topic that is ripe for new discoveries. They benefit from the abundant synthetic methods, optional chemical compositions, and emerging nanotechnologies, and offer a great opportunity to explore materials with extraordinary properties. For example, the combination of porous polyelectrolytes with polymer processing technologies and chemical methods for porous polymers (3D printing,[107] microfluidics,[108] wet/electrospinning,[109] polymers of intrinsic microporosity,[86] and conjugated microporous polymers,[110] etc.) brings exciting opportunities but is still in its infancy. We can foresee porous polyelectrolytes unceasingly initiating the interest and curiosity of scientists and even leading to the production of fine products in industry.

Acknowledgements

Q.Z. thanks funding support from the Huazhong University of Science and Technology (No. 3004013118) and the 1000 Young Talent program. J.Y. thanks Clarkson University for a startup grant. Part of this work is supported by an ERC starting grant (project 639720-NAPOLI).

Conflict of interest

The authors declare no conflict of interest.

How to cite: *Angew. Chem. Int. Ed.* **2018**, *57*, 6754 – 6773
Angew. Chem. **2018**, *130*, 6868 – 6889

[1] a) A. G. Slater, A. I. Cooper, *Science* **2015**, *348*, aaa8075; b) D. C. Wu, F. Xu, B. Sun, R. W. Fu, H. K. He, K. Matyjaszewski, *Chem. Rev.* **2012**, *112*, 3959 – 4015.
[2] M. A. Shannon, P. W. Bohn, M. Elimelech, J. G. Georgiadis, B. J. Marinas, A. M. Mayes, *Nature* **2008**, *452*, 301 – 310.
[3] a) M. T. Gokmen, F. E. Du Prez, *Prog. Polym. Sci.* **2012**, *37*, 365 – 405; b) Y. G. Zhang, S. N. Riduan, *Chem. Soc. Rev.* **2012**, *41*, 2083 – 2094; c) A. Muñoz-Bonilla, M. Fernandez-García, J. Rodríguez-Hernández, *Prog. Polym. Sci.* **2014**, *39*, 510 – 554; d) M. S. Silverstein, *Prog. Polym. Sci.* **2014**, *39*, 199 – 234; e) A. G. Fane, R. Wang, M. X. Hu, *Angew. Chem. Int. Ed.* **2015**, *54*, 3368 – 3386; *Angew. Chem.* **2015**, *127*, 3427 – 3447; f) W. Mai, B. Sun, L. Chen, F. Xu, H. Liu, Y. Liang, R. Fu, D. Wu, K. Matyjaszewski, *J. Am. Chem. Soc.* **2015**, *137*, 13256 – 13259; g) J. Yuan, M. Drechsler, Y. Xu, M. Zhang, A. H. E. Müller, *Polymer* **2008**, *49*, 1547 – 1554.
[4] a) A. V. Dobrynin, M. Rubinstein, *Prog. Polym. Sci.* **2005**, *30*, 1049 – 1118; b) J. Lu, F. Yan, J. Texter, *Prog. Polym. Sci.* **2009**, *34*, 431 – 448; c) J. Yuan, D. Mecerreyes, M. Antonietti, *Prog. Polym. Sci.* **2013**, *38*, 1009 – 1036; d) W. Qian, J. Texter, F. Yan, *Chem. Soc. Rev.* **2017**, *46*, 1124 – 1159.
[5] a) N. N. Li, A. G. Fane, W. S. Ho, T. Matsuura, *Advanced Membrane Technology & Applications*, Wiley, Hoboken, **2008**; b) M. Mulder, *Basic Principles of Membrane Technology*, 2nd edition, Kluwer, Dordrecht, **1998**.
[6] a) M. Mulder, *Basic Principles of Membrane Technology*, 2nd edition, Kluwer, Dordrecht, **1998**; b) M. B. Larsen, J. D. Van Horn, F. Wu, M. A. Hillmyer, *Macromolecules* **2017**, *50*, 4363 – 4371.
[7] a) P. Zhang, M. Li, B. Yang, Y. Fang, X. Jiang, G. M. Veith, X.-G. Sun, S. Dai, *Adv. Mater.* **2015**, *27*, 8088 – 8094; b) S. Zhang, K. Ueno, K. Dokko, M. Watanabe, *Adv. Energy Mater.* **2015**, *5*, 1500117.
[8] a) J. Cui, J. J. Richardson, M. Björnmalm, M. Faria, F. Caruso, *Acc. Chem. Res.* **2016**, *49*, 1139 – 1148; b) M. W. Amjad, P. Kesharwani, M. C. I. Mohd Amin, A. K. Iyer, *Prog. Polym. Sci.* **2017**, *64*, 154 – 181.
[9] a) L. Tan, B. Tan, *Chem. Soc. Rev.* **2017**, *46*, 3322 – 3356; b) J.-K. Sun, M. Antonietti, J. Yuan, *Chem. Soc. Rev.* **2016**, *45*, 6627 – 6656; c) C. Perego, R. Millini, *Chem. Soc. Rev.* **2013**, *42*, 3956 – 3976; d) M. E. Davis, *Nature* **2002**, *417*, 813 – 821; e) A. H. Lu, F. Schüth, *Adv. Mater.* **2006**, *18*, 1793 – 1805; f) S. Das, P. Heasman, T. Ben, S. Qiu, *Chem. Rev.* **2017**, *117*, 1515 – 1563; g) S. G. Zhang, K. Dokko, M. Watanabe, *Chem. Sci.* **2015**, *6*, 3684 – 3691.
[10] I. Tokarev, S. Minko, *Adv. Mater.* **2009**, *21*, 241 – 247.
[11] M. C. Berg, L. Zhai, R. E. Cohen, M. F. Rubner, *Biomacromolecules* **2006**, *7*, 357 – 364.
[12] a) I. Tokarev, S. Minko, *Soft Matter* **2009**, *5*, 511 – 524; b) I. Tokarev, S. Minko, *Adv. Mater.* **2010**, *22*, 3446 – 3462.
[13] M. S. Islam, W. S. Choi, H. J. Lee, Y. B. Lee, I. C. Jeon, *J. Mater. Chem.* **2012**, *22*, 8215 – 8220.
[14] a) T. Crouzier, F. Sailhan, P. Becquart, R. Guillot, D. Logeart-Avramoglou, C. Picart, *Biomaterials* **2011**, *32*, 7543 – 7554; b) E. S. Dragan, F. Bucatariu, G. Hitruc, *Biomacromolecules* **2010**, *11*, 787 – 796.
[15] G. Decher, *Science* **1997**, *277*, 1232 – 1237.
[16] J. J. Richardson, M. Bjornmalm, F. Caruso, *Science* **2015**, *348*, aaa2491.
[17] Q. Zhao, Q. F. An, Y. L. Ji, J. W. Qian, C. J. Gao, *J. Membr. Sci.* **2011**, *379*, 19 – 45.
[18] J. D. Mendelsohn, C. J. Barrett, V. V. Chan, A. J. Pal, A. M. Mayes, M. F. Rubner, *Langmuir* **2000**, *16*, 5017 – 5023.
[19] a) J. Hiller, J. D. Mendelsohn, M. F. Rubner, *Nat. Mater.* **2002**, *1*, 59 – 63; b) F. C. Cebeci, Z. Z. Wu, L. Zhai, R. E. Cohen, M. F. Rubner, *Langmuir* **2006**, *22*, 2856 – 2862; c) L. Zhai, A. J. Nolte, R. E. Cohen, M. F. Rubner, *Macromolecules* **2004**, *37*, 6113 – 6123; d) D. Lee, A. J. Nolte, A. L. Kunz, M. F. Rubner, R. E. Cohen, *J. Am. Chem. Soc.* **2006**, *128*, 8521 – 8529; e) J. Bravo, L. Zhai, Z. Z. Wu, R. E. Cohen, M. F. Rubner, *Langmuir* **2007**, *23*, 7293 – 7298; f) C. S. Hajicharalambous, J. Lichter, W. T. Hix, M. Swierczewska, M. F. Rubner, P. Rajagopalan, *Biomaterials* **2009**, *30*, 4029 – 4036.
[20] a) A. Fery, B. Scholer, T. Cassagneau, F. Caruso, *Langmuir* **2001**, *17*, 3779 – 3783; b) Z. L. Gui, J. W. Qian, M. J. Yin, Q. F. An, B. B. Gu, A. Zhang, *J. Mater. Chem.* **2010**, *20*, 7754 – 7760.
[21] C. Cho, J. W. Jeon, J. Lutkenhaus, N. S. Zacharia, *ACS Appl. Mater. Interfaces* **2013**, *5*, 4930 – 4936.
[22] C. Li, K. Wang, Y. H. Gong, Z. Y. Li, J. Zhang, G. F. Luo, R. X. Zhuo, X. Z. Zhang, *J. Mater. Chem.* **2012**, *22*, 2045 – 2050.
[23] Q. Li, J. F. Quinn, F. Caruso, *Adv. Mater.* **2005**, *17*, 2058 – 2062.
[24] X. L. Chen, J. Q. Sun, *Chem. Asian J.* **2014**, *9*, 2063 – 2067.
[25] a) J. Yu, S. Y. Han, J. S. Hong, O. Sanyal, I. Lee, *Langmuir* **2016**, *32*, 8494 – 8500; b) J. Yu, O. Sanyal, A. P. Izbicki, I. Lee, *Macromol. Rapid Commun.* **2015**, *36*, 1669 – 1674; c) J. Yu, B. M. Meharg, I. Lee, *Polymer* **2017**, *109*, 297 – 306.
[26] Y. Fu, S. L. Bai, S. X. Cui, D. L. Qiu, Z. Q. Wang, X. Zhang, *Macromolecules* **2002**, *35*, 9451 – 9458.
[27] S. L. Bai, Z. Q. Wang, X. Zhang, B. Wang, *Langmuir* **2004**, *20*, 11828 – 11832.

[28] a) S. L. Bai, Z. Q. Wang, J. Gao, X. Zhang, *Eur. Polym. J.* **2006**, *42*, 900 – 907; b) Q. Shao, S. Y. Jiang, *Adv. Mater.* **2015**, *27*, 15 – 26.

[29] Z. L. Gui, J. W. Qian, Y. He, Q. F. An, X. S. Wang, C. P. Tian, W. D. Sun, *J. Colloid Interface Sci.* **2011**, *361*, 122 – 128.

[30] J. L. Zou, F. Kim, *Nat. Commun.* **2014**, *5*, 5254.

[31] a) Y. Li, S. S. Chen, M. C. Wu, J. Q. Sun, *Adv. Mater.* **2014**, *26*, 3344 – 3348; b) L. Zhang, M. A. Zheng, X. K. Liu, J. Q. Sun, *Langmuir* **2011**, *27*, 1346 – 1352.

[32] a) Q. Zhao, J. W. Qian, Q. F. An, B. Y. Du, *J. Mater. Chem.* **2009**, *19*, 8448 – 8455; b) Q. Zhao, J. W. Qian, Q. F. An, Z. W. Sun, *J. Membr. Sci.* **2010**, *346*, 335 – 343.

[33] a) J. Chen, X. M. Xia, S. W. Huang, R. X. Zhuo, *Adv. Mater.* **2007**, *19*, 979 – 983; b) N. Peng, X. M. Xia, W. T. He, W. M. Liu, S. W. Huang, R. X. Zhuo, *Polymer* **2011**, *52*, 1256 – 1262.

[34] T. Ogoshi, S. Takashima, T. A. Yamagishi, *J. Am. Chem. Soc.* **2015**, *137*, 10962 – 10964.

[35] a) T. Mitra, K. E. Jelfs, M. Schmidtmann, A. Ahmed, S. Y. Chong, D. J. Adams, A. I. Cooper, *Nat. Chem.* **2013**, *5*, 276 – 281; b) Z. B. Zhang, Q. Zhao, J. Y. Yuan, M. Antonietti, F. H. Huang, *Chem. Commun.* **2014**, *50*, 2595 – 2597; c) K.-D. Zhang, J. Tian, D. Hanifi, Y. Zhang, A. C.-H. Sue, T.-Y. Zhou, L. Zhang, X. Zhao, Y. Liu, Z.-T. Li, *J. Am. Chem. Soc.* **2013**, *135*, 17913 – 17918; d) M. Pfeffermann, R. Dong, R. Graf, W. Zajaczkowski, T. Gorelik, W. Pisula, A. Narita, K. Müllen, X. Feng, *J. Am. Chem. Soc.* **2015**, *137*, 14525 – 14532.

[36] a) A. J. Zhang, H. Bai, L. Li, *Chem. Rev.* **2015**, *115*, 9801 – 9868; b) L. S. Wan, L. W. Zhu, Y. Ou, Z. K. Xu, *Chem. Commun.* **2014**, *50*, 4024 – 4039.

[37] a) D. Beattie, K. H. Wong, C. Williams, L. A. Poole-Warren, T. P. Davis, C. Barner-Kowollik, M. H. Stenzel, *Biomacromolecules* **2006**, *7*, 1072 – 1082; b) T. Kabuto, Y. Hashimoto, O. Karthaus, *Adv. Funct. Mater.* **2007**, *17*, 3569 – 3573; c) C. Y. Wang, Y. D. Mao, D. Y. Wang, Q. S. Qu, G. J. Yang, X. Y. Hu, *J. Mater. Chem.* **2008**, *18*, 683 – 690; d) L. Li, C. K. Chen, A. J. Zhang, X. Y. Liu, K. Cui, J. Huang, Z. Ma, Z. H. Han, *J. Colloid Interface Sci.* **2009**, *331*, 446 – 452; e) L. Li, Y. W. Zhong, C. Y. Ma, J. Li, C. K. Chen, A. J. Zhang, D. L. Tang, S. Y. Xie, Z. Ma, *Chem. Mater.* **2009**, *21*, 4977 – 4983; f) L. Li, Y. W. Zhong, J. L. Gong, J. A. Li, C. K. Chen, B. R. Zeng, Z. Ma, *Soft Matter* **2011**, *7*, 546 – 552; g) J. Y. Ding, J. L. Gong, H. Bai, L. Li, Y. W. Zhong, Z. Ma, V. Svrcek, *J. Colloid Interface Sci.* **2012**, *380*, 99 – 104; h) J. L. Gong, L. C. Sun, Y. W. Zhong, C. Y. Ma, L. Li, S. Y. Xie, V. Svrcek, *Nanoscale* **2012**, *4*, 278 – 283.

[38] a) H. Sai, K. W. Tan, K. Hur, E. Asenath-Smith, R. Hovden, Y. Jiang, M. Riccio, D. A. Muller, V. Elser, L. A. Estroff, S. M. Gruner, U. Wiesner, *Science* **2013**, *341*, 530 – 534; b) K. W. Tan, B. Jung, J. G. Werner, E. R. Rhoades, M. O. Thompson, U. Wiesner, *Science* **2015**, *349*, 54 – 58.

[39] a) J. Li, J. T. Cheng, Y. Zhang, P. Gopalakrishnakone, *Colloid Polym. Sci.* **2009**, *287*, 29 – 36; b) P. Escalé, L. Rubatat, C. Derail, M. Save, L. Billon, *Macromol. Rapid Commun.* **2011**, *32*, 1072 – 1076.

[40] X. Y. Li, Q. L. Zhao, T. T. Xu, J. Huang, L. H. Wei, Z. Ma, *Eur. Polym. J.* **2014**, *50*, 135 – 141.

[41] a) S. P. Nunes, R. Sougrat, B. Hooghan, D. H. Anjum, A. R. Behzad, L. Zhao, N. Pradeep, I. Pinnau, U. Vainio, K. V. Peinemann, *Macromolecules* **2010**, *43*, 8079 – 8085; b) S. P. Nunes, A. R. Behzad, B. Hooghan, R. Sougrat, M. Karunakaran, N. Pradeep, U. Vainio, K. V. Peinemann, *ACS Nano* **2011**, *5*, 3516 – 3522; c) H. Z. Yu, X. Y. Qiu, S. P. Nunes, K. V. Peinemann, *Angew. Chem. Int. Ed.* **2014**, *53*, 10072 – 10076; *Angew. Chem.* **2014**, *126*, 10236 – 10240; d) X. Y. Qiu, H. Z. Yu, M. Karunakaran, N. Pradeep, S. P. Nunes, K. V. Peinemann, *Acs Nano* **2013**, *7*, 768 – 776; e) K. V. Peinemann, V. Abetz, P. F. W. Simon, *Nat. Mater.* **2007**, *6*, 992 – 996; f) J. Hahn, J. I. Clodt, C. Abetz, V. Filiz, V. Abetz, *ACS Appl. Mater. Interfaces* **2015**, *7*, 21130 – 21137; g) M. Radjabian, V. Abetz, *Adv. Mater.* **2015**, *27*, 352 – 355; h) V. Abetz, *Macromol. Rapid Commun.* **2015**, *36*, 10 – 22.

[42] a) D. L. Gin, R. D. Noble, *Science* **2011**, *332*, 674 – 676; b) R. D. Noble, D. L. Gin, *J. Membr. Sci.* **2011**, *369*, 1 – 4; c) S. Zulfiqar, M. I. Sarwar, D. Mecerreyes, *Polym. Chem.* **2015**, *6*, 6435 – 6451.

[43] a) D. I. Mori, R. M. Martin, R. D. Noble, D. L. Gin, *Polymer* **2017**, *112*, 435 – 446; b) R. L. Kerr, J. P. Edwards, S. C. Jones, B. J. Elliott, D. L. Gin, *Polym. J.* **2016**, *48*, 635 – 643; c) M. Yoshio, T. Kagata, K. Hoshino, T. Mukai, H. Ohno, T. Kato, *J. Am. Chem. Soc.* **2006**, *128*, 5570 – 5577; d) K. M. Meek, S. Sharick, Y. S. Ye, K. I. Winey, Y. A. Elabd, *Macromolecules* **2015**, *48*, 4850 – 4862; e) G. E. Sanoja, B. C. Popere, B. S. Beckingham, C. M. Evans, N. A. Lynd, R. A. Segalman, *Macromolecules* **2016**, *49*, 2216 – 2223; f) J. H. Choi, W. Xie, Y. Y. Gu, C. D. Frisbie, T. P. Lodge, *ACS Appl. Mater. Interfaces* **2015**, *7*, 7294 – 7302.

[44] a) F. Yan, J. Texter, *Angew. Chem. Int. Ed.* **2007**, *46*, 2440 – 2443; *Angew. Chem.* **2007**, *119*, 2492 – 2495; b) D. England, F. Yan, J. Texter, *Langmuir* **2013**, *29*, 12013 – 12024; c) H. Gu, J. Texter, *Polymer* **2014**, *55*, 3378 – 3384; d) D. England, N. Tambe, J. Texter, *Acs Macro Lett.* **2012**, *1*, 310 – 314; e) Y. Ren, J. Zhang, J. Guo, F. Chen, F. Yan, *Macromol. Rapid Commun.* **2017**, *38*, 1700151; f) Z. Qiu, J. Texter, *Curr. Opin. Colloid Interface Sci.* **2008**, *13*, 252 – 262; g) F. Yan, J. Texter, *Soft Matter* **2006**, *2*, 109 – 118; h) K. A. Page, D. England, J. Texter, *Acs Macro Lett.* **2012**, *1*, 1398 – 1402; i) J. Texter, *Macromol. Rapid Commun.* **2012**, *33*, 1996 – 2014; j) F. Yan, J. Texter, *Chem. Commun.* **2006**, 2696 – 2698.

[45] a) Q. Zhao, M. J. Yin, A. P. Zhang, S. Prescher, M. Antonietti, J. Y. Yuan, *J. Am. Chem. Soc.* **2013**, *135*, 5549 – 5552; b) Q. Zhao, J. W. C. Dunlop, X. L. Qiu, F. H. Huang, Z. B. Zhang, J. Heyda, J. Dzubiella, M. Antonietti, J. Y. Yuan, *Nat. Commun.* **2014**, *5*, 4293; c) Q. Zhao, J. Heyda, J. Dzubiella, K. Tauber, J. W. C. Dunlop, J. Y. Yuan, *Adv. Mater.* **2015**, *27*, 2913 – 2917; d) K. Täuber, B. Lepenies, J. Y. Yuan, *Polym. Chem.* **2015**, *6*, 4855 – 4858; e) K. Täuber, Q. Zhao, M. Antonietti, J. Y. Yuan, *Acs Macro Lett.* **2015**, *4*, 39 – 42; f) K. Täuber, A. Dani, J. Yuan, *Acs Macro Lett.* **2017**, *6*, 1 – 5; g) Q. Zhao, P. Zhang, M. Antonietti, J. Yuan, *J. Am. Chem. Soc.* **2012**, *134*, 11852 – 11855.

[46] a) A. Wilke, J. Y. Yuan, M. Antonietti, J. Weber, *ACS Macro Lett.* **2012**, *1*, 1028 – 1031; b) X. B. Hu, J. Huang, W. X. Zhang, M. Li, C. G. Tao, G. T. Li, *Adv. Mater.* **2008**, *20*, 4074 – 4078; c) J. Huang, C. A. Tao, Q. An, C. X. Lin, X. S. Li, D. Xu, Y. G. Wu, X. G. Li, D. Z. Shen, G. T. Li, *Chem. Commun.* **2010**, *46*, 4103 – 4105; d) J. Huang, C. A. Tao, Q. An, W. X. Zhang, Y. G. Wu, X. S. Li, D. Z. Shen, G. T. Li, *Chem. Commun.* **2010**, *46*, 967 – 969; e) J. C. Cui, W. Zhu, N. Gao, J. Li, H. W. Yang, Y. Jiang, P. Seidel, B. J. Ravoo, G. T. Li, *Angew. Chem. Int. Ed.* **2014**, *53*, 3844 – 3848; *Angew. Chem.* **2014**, *126*, 3923 – 3927.

[47] L. Qin, B. Wang, Y. Zhang, L. Chen, G. Gao, *Chem. Commun.* **2017**, *53*, 3785 – 3788.

[48] K. Täuber, A. Dani, J. Y. Yuan, *ACS Macro Lett.* **2017**, *6*, 1 – 5.

[49] a) K. Täuber, A. Zimathies, J. Y. Yuan, *Macromol. Rapid Commun.* **2015**, *36*, 2176 – 2180; b) Q. Zhao, D. W. Lee, B. K. Ahn, S. Seo, Y. Kaufman, J. N. Israelachvili, J. H. Waite, *Nat. Mater.* **2016**, *15*, 407 – 412.

[50] K. H. Zhang, X. L. Feng, X. F. Sui, M. A. Hempenius, G. J. Vancso, *Angew. Chem. Int. Ed.* **2014**, *53*, 13789 – 13793; *Angew. Chem.* **2014**, *126*, 14009 – 14013.

[51] a) L. Ge, A. N. Mondal, X. Liu, B. Wu, D. Yu, Q. Li, J. Miao, Q. Ge, T. Xu, *J. Membr. Sci.* **2017**, *536*, 11 – 18; b) X. Lin, E. Shamsaei, B. Kong, J. Z. Liu, D. Zhao, T. Xu, Z. Xie, C. D. Easton, H. Wang, *J. Membr. Sci.* **2016**, *510*, 437 – 446; c) E. Bakangura, C. Cheng, L. Wu, X. Ge, J. Ran, M. I. Khan, E. Kamana, N. Afsar, M. Irfan, A. Shehzad, T. Xu, *J. Membr. Sci.* **2017**, *537*, 32 – 41; d) E. Bakangura, C. Cheng, L. Wu, Y. He, X.

Ge, J. Ran, K. Emmanuel, T. Xu, *J. Membr. Sci.* **2016**, *515*, 154 – 162; e) A. L. Wu, F. Lu, M. W. Zhao, N. Sun, L. J. Shi, L. Q. Zheng, *ChemistrySelect* **2017**, *2*, 1878 – 1884.

[52] Y. Q. Yang, Q. F. Zhang, S. H. Li, S. B. Zhang, *RSC Adv.* **2015**, *5*, 3567 – 3573.

[53] a) J. R. Slotkin, C. D. Pritchard, B. Luque, J. Ye, R. T. Layer, M. S. Lawrence, T. M. O'Shea, R. R. Roy, H. Zhong, I. Vollenweider, V. R. Edgerton, G. Courtine, E. J. Woodard, R. Langer, *Biomaterials* **2017**, *123*, 63 – 76; b) D. F. Coutinho, S. Sant, M. Shakiba, B. Wang, M. E. Gomes, N. M. Neves, R. L. Reis, A. Khademhosseini, *J. Mater. Chem.* **2012**, *22*, 17262 – 17271.

[54] Y. Si, L. Wang, X. Wang, N. Tang, J. Yu, B. Ding, *Adv. Mater.* **2017**, *29*, 1700339.

[55] S. J. Florczyk, D. J. Kim, D. L. Wood, M. Q. Zhang, *J. Biomed. Mater. Res. Part A* **2011**, *98*, 614 – 620.

[56] a) F. M. Kievit, S. J. Florczyk, M. C. Leung, O. Veiseh, J. O. Park, M. L. Disis, M. Q. Zhang, *Biomaterials* **2010**, *31*, 5903 – 5910; b) Z. S. Li, H. R. Ramay, K. D. Hauch, D. M. Xiao, M. Q. Zhang, *Biomaterials* **2005**, *26*, 3919 – 3928; c) Z. S. Li, M. Q. Zhang, *J. Biomed. Mater. Res. Part A* **2005**, *75*, 485 – 493; d) H. R. Ramay, Z. S. Li, E. Shum, M. Q. Zhang, *J. Biomed. Nanotechnol.* **2005**, *1*, 151 – 160; e) M. Leung, F. M. Kievit, S. J. Florczyk, O. Veiseh, J. Wu, J. O. Park, M. Q. Zhang, *Pharm. Res.* **2010**, *27*, 1939 – 1948; f) S. H. Hsu, S. W. Whu, S. C. Hsieh, C. L. Tsai, D. C. Chen, T. S. Tan, *Artif. Organs* **2004**, *28*, 693 – 703; g) B. W. Yao, H. Y. Wang, Q. Q. Zhou, M. M. Wu, M. Zhang, C. Li, G. C. Shi, *Adv. Mater.* **2017**, *29*, 1700974; h) J. Yang, T. W. Chung, M. Nagaoka, M. Goto, C. S. Cho, T. Akaike, *Biotechnol. Lett.* **2001**, *23*, 1385 – 1389; i) B. De la Riva, C. Nowak, E. Sanchez, A. Hernandez, M. Schulz-Siegmund, M. K. Pec, A. Delgado, C. Evora, *Eur. J. Pharm. Biopharm.* **2009**, *73*, 50 – 58; j) J. Han, Z. Y. Zhou, R. X. Yin, D. Z. Yang, J. Nie, *Int. J. Biol. Macromol.* **2010**, *46*, 199 – 205; k) Y. C. Ho, F. L. Mi, H. W. Sung, P. L. Kuo, *Int. J. Pharm.* **2009**, *376*, 69 – 75; l) H. Y. Lin, C. T. Yeh, *J. Mater. Sci. Mater. Med.* **2010**, *21*, 1611 – 1620; m) R. S. Tığlı, M. Gümüşderelioğlu, *J. Mater. Sci. Mater. Med.* **2009**, *20*, 699 – 709; n) S. S. Olmez, P. Korkusuz, H. Bilgili, S. Senel, *Pharmazie* **2007**, *62*, 423 – 431; o) X. X. Li, H. G. Xie, J. Z. Lin, W. Y. Xie, X. J. Ma, *Polym. Degrad. Stab.* **2009**, *94*, 1 – 6.

[57] a) D. Verma, K. S. Katti, D. R. Katti, *Philos. Trans. R. Soc. A* **2010**, *368*, 2083 – 2097; b) D. Verma, K. S. Katti, D. R. Katti, *Mater. Sci. Eng. C* **2009**, *29*, 2079 – 2084.

[58] a) H. D. Wu, J. C. Yang, T. Tsai, D. Y. Ji, W. J. Chang, C. C. Chen, S. Y. Lee, *Carbohydr. Polym.* **2011**, *85*, 318 – 324; b) H. D. Wu, D. Y. Ji, W. J. Chang, J. C. Yang, S. Y. Lee, *Mater. Sci. Eng.* **2012**, *32*, 207 – 214.

[59] H. Q. Chen, M. W. Fan, *J. Bioact. Compat. Polym. Pol.* **2007**, *22*, 475 – 491.

[60] a) Z. D. She, C. R. Jin, Z. Huang, B. F. Zhang, Q. L. Feng, Y. X. Xu, *J. Mater. Sci.* **2008**, *19*, 3545 – 3553; b) A. S. Gobin, V. E. Froude, A. B. Mathur, *J. Biomed. Mater. Res. Part A* **2005**, *74*, 465 – 473; c) N. Bhardwaj, S. C. Kundu, *Carbohydr. Polym.* **2011**, *85*, 325 – 333.

[61] P. Coimbra, P. Alves, T. A. M. Valente, R. Santos, I. J. Correia, P. Ferreira, *Int. J. Biol. Macromol.* **2011**, *49*, 573 – 579.

[62] P. Coimbra, P. Ferreira, H. C. de Sousa, P. Batista, M. A. Rodrigues, I. J. Corriea, M. H. Gil, *Int. J. Biol. Macromol.* **2011**, *48*, 112 – 118.

[63] a) A. Reisch, P. Tirado, E. Roger, F. Boulmedais, D. Collin, J. C. Voegel, B. Frisch, P. Schaaf, J. B. Schlenoff, *Adv. Funct. Mater.* **2013**, *23*, 673 – 682; b) R. A. Ghostine, R. F. Shamoun, J. B. Schlenoff, *Macromolecules* **2013**, *46*, 4089 – 4094; c) R. F. Shamoun, H. H. Hariri, R. A. Ghostine, J. B. Schlenoff, *Macromolecules* **2012**, *45*, 9759 – 9767; d) R. F. Shamoun, A. Reisch, J. B. Schlenoff, *Adv. Funct. Mater.* **2012**, *22*, 1923 – 1931; e) C. H. Porcel, J. B. Schlenoff, *Biomacromolecules* **2009**, *10*, 2968 – 2975; f) P. Tirado, A. Reisch, E. Roger, F. Boulmedais, L. Jierry, P. Lavalle, J. C. Voegel, P. Schaaf, J. B. Schlenoff, B. Frisch, *Adv. Funct. Mater.* **2013**, *23*, 4785 – 4792; g) H. H. Hariri, J. B. Schlenoff, *Macromolecules* **2010**, *43*, 8656 – 8663; h) A. Reisch, E. Roger, T. Phoeung, C. Antheaume, C. Orthlieb, F. Boulmedais, P. Lavalle, J. B. Schlenoff, B. Frisch, P. Schaaf, *Adv. Mater.* **2014**, *26*, 2547 – 2551.

[64] P. Schaaf, J. B. Schlenoff, *Adv. Mater.* **2015**, *27*, 2420 – 2432.

[65] a) Y. Yan, Z. W. Lai, R. J. A. Goode, J. W. Cui, T. Bacic, M. M. J. Kamphuis, E. C. Nice, F. Caruso, *ACSs Nano* **2013**, *7*, 5558 – 5567; b) Y. Yan, G. K. Such, A. P. R. Johnston, J. P. Best, F. Caruso, *ACS Nano* **2012**, *6*, 3663 – 3669; c) J. W. Cui, Y. Yan, Y. J. Wang, F. Caruso, *Adv. Funct. Mater.* **2012**, *22*, 4718 – 4723; d) J. Tan, Y. J. Wang, X. P. Yip, F. Glynn, R. K. Shepherd, F. Caruso, *Adv. Mater.* **2012**, *24*, 3362 – 3366; e) Y. J. Wang, F. Caruso, *Adv. Mater.* **2006**, *18*, 795 – 800; f) Y. J. Wang, Y. Yan, J. W. Cui, L. Hosta-Rigau, J. K. Heath, E. C. Nice, F. Caruso, *Adv. Mater.* **2010**, *22*, 4293 – 4297; g) Y. J. Wang, A. M. Yu, F. Caruso, *Angew. Chem. Int. Ed.* **2005**, *44*, 2888 – 2892; *Angew. Chem.* **2005**, *117*, 2948 – 2952; h) X. H. Yan, J. B. Li, H. Mohwald, *Adv. Mater.* **2012**, *24*, 2663 – 2667; i) Q. L. Zou, L. Zhang, X. H. Yan, A. H. Wang, G. H. Ma, J. B. Li, H. Mohwald, S. Mann, *Angew. Chem. Int. Ed.* **2014**, *53*, 2366 – 2370; *Angew. Chem.* **2014**, *126*, 2398 – 2402.

[66] H. Z. Yu, X. Y. Qiu, S. P. Nunes, K. V. Peinemann, *Nat. Commun.* **2014**, *5*, 4110.

[67] a) C. J. Gao, G. J. Chen, X. C. Wang, J. Li, Y. Zhou, J. Wang, *Chem. Commun.* **2015**, *51*, 4969 – 4972; b) I. Azcune, I. Garcia, P. M. Carrasco, A. Genua, M. Tanczyk, M. Jaschik, K. Warmuzinski, G. Cabanero, I. Odriozola, *ChemSusChem* **2014**, *7*, 3407 – 3412; c) C. Boyère, A. Favrelle, A. F. Léonard, F. Boury, C. Jérôme, A. Debuigne, *J. Mater. Chem. A* **2013**, *1*, 8479 – 8487.

[68] a) Q. Zhao, S. Soll, M. Antonietti, J. Y. Yuan, *Polym. Chem.* **2013**, *4*, 2432 – 2435; b) S. Soll, P. F. Zhang, Q. Zhao, Y. Wang, J. Y. Yuan, *Polym. Chem.* **2013**, *4*, 5048 – 5051; c) S. Soll, Q. Zhao, J. Weber, J. Y. Yuan, *Chem. Mater.* **2013**, *25*, 3003 – 3010.

[69] a) D. Kuzmicz, P. Coupillaud, Y. Men, J. Vignolle, G. Vendraminetto, M. Ambrogi, D. Taton, J. Y. Yuan, *Polymer* **2014**, *55*, 3423 – 3430; b) A. Dani, E. Groppo, C. Barolo, J. G. Vitillo, S. Bordiga, *J. Mater. Chem. A* **2015**, *3*, 8508 – 8518; c) X. C. Wang, J. Li, G. J. Chen, Z. J. Guo, Y. Zhou, J. Wang, *ChemCatChem* **2015**, *7*, 993 – 1003; d) X. P. Feng, C. J. Gao, Z. J. Guo, Y. Zhou, J. Wang, *RSC Adv.* **2014**, *4*, 23389 – 23395; e) F. J. Liu, L. Wang, Q. Sun, L. F. Zhu, X. J. Meng, F. S. Xiao, *J. Am. Chem. Soc.* **2012**, *134*, 16948 – 16950; f) C.-X. Cao, J. Yuan, J.-P. Cheng, B.-H. Han, *Sci. Rep.* **2017**, *7*, 3101.

[70] P. Zhang, X. Jiang, S. Wan, S. Dai, *Chem. Eur. J.* **2015**, *21*, 12866 – 12870.

[71] A. Dani, V. Crocella, C. Magistris, V. Santoro, J. Y. Yuan, S. Bordiga, *J. Mater. Chem. A* **2017**, *5*, 372 – 383.

[72] J. X. Han, Z. J. Du, W. Zou, H. Q. Li, C. Zhang, *J. Hazard. Mater.* **2014**, *276*, 225 – 231.

[73] X. Liu, H. Chen, C. H. Wang, R. J. Qu, C. N. Ji, C. M. Sun, Y. Zhang, *J. Hazard. Mater.* **2010**, *175*, 1014 – 1021.

[74] J. H. Chen, H. T. Xing, H. X. Guo, G. P. Li, W. Weng, S. R. Hu, *J. Hazard. Mater.* **2013**, *248*, 285 – 294.

[75] G. Barin, G. W. Peterson, V. Crocella, J. Xu, K. A. Colwell, A. Nandy, J. A. Reimer, S. Bordiga, J. R. Long, *Chem. Sci.* **2017**, *8*, 4399 – 4409.

[76] a) I. Tokarev, V. Gopishetty, S. Minko, *Acs Appl. Mater. Interfaces* **2015**, *7*, 12463 – 12469; b) J. B. Qu, L. Y. Chu, M. Yang, R. Xie, L. Hu, W. M. Chen, *Adv. Funct. Mater.* **2006**, *16*, 1865 – 1872; c) V. Gopishetty, Y. Roiter, I. Tokarev, S. Minko, *Adv. Mater.* **2008**, *20*, 4588 – 4593.

[77] Y. B. Gu, U. Wiesner, *Macromolecules* **2015**, *48*, 6153 – 6159.

[78] Y. B. Gu, R. M. Dorin, U. Wiesner, *Nano Lett.* **2013**, *13*, 5323 – 5328.
[79] B. P. Tripathi, N. C. Dubey, S. Choudhury, P. Formanek, M. Stamm, *Adv. Mater. Interfaces* **2015**, *2*, 1500097.
[80] H. Kuroki, C. Islam, I. Tokarev, H. Hu, G. J. Liu, S. Minko, *ACS Appl. Mater. Interfaces* **2015**, *7*, 10401 – 10406.
[81] M. Joo, J. Shin, J. Kim, J. B. You, Y. Yoo, M. J. Kwak, M. S. Oh, S. G. Im, *J. Am. Chem. Soc.* **2017**, *139*, 2329 – 2337.
[82] a) Y. Z. Zhu, F. Zhang, D. Wang, X. F. Pei, W. B. Zhang, J. Jin, *J. Mater. Chem. A* **2013**, *1*, 5758 – 5765; b) Y. Z. Zhu, W. Xie, F. Zhang, T. L. Xing, J. Jin, *ACS Appl. Mater. Interfaces* **2017**, *9*, 9603 – 9613; c) K. He, H. R. Duan, G. Y. Chen, X. K. Liu, W. S. Yang, D. Y. Wang, *ACS Nano* **2015**, *9*, 9188 – 9198.
[83] a) L. Folkertsma, K. H. Zhang, O. Czakkel, H. L. de Boer, M. A. Hempenius, A. van den Berg, M. Odijk, G. J. Vancso, *Macromolecules* **2017**, *50*, 296 – 302; b) H. Lin, J. Gong, H. Miao, R. Guterman, H. Song, Q. Zhao, J. W. C. Dunlop, J. Yuan, *ACS Appl. Mater. Interfaces* **2017**, *9*, 15148 – 15155; c) J.-K. Sun, H.-J. Lin, W.-Y. Zhang, M.-R. Gao, M. Antonietti, J. Yuan, *Mater. Horiz.* **2017**, *4*, 681 – 687.
[84] a) H. Wang, S. X. Min, C. Ma, Z. X. Liu, W. Y. Zhang, Q. Wang, D. B. Li, Y. Y. Li, S. Turner, Y. Han, H. B. Zhu, E. Abou-Hamad, M. N. Hedhili, J. Pan, W. L. Yu, K. W. Huang, L. J. Li, J. Y. Yuan, M. Antonietti, T. Wu, *Nat. Commun.* **2017**, *8*, 13592; b) H. Wang, S. Min, Q. Wang, D. Li, G. Casillas, C. Ma, Y. Li, Z. Liu, L.-J. Li, J. Yuan, M. Antonietti, T. Wu, *ACS Nano* **2017**, *11*, 4358 – 4364; c) H. Wang, J. Jia, P. Song, Q. Wang, D. Li, S. Min, C. Qian, L. Wang, Y. F. Li, C. Ma, T. Wu, J. Yuan, M. Antonietti, G. A. Ozin, *Angew. Chem. Int. Ed.* **2017**, *56*, 7847 – 7852; *Angew. Chem.* **2017**, *129*, 7955 – 7960.
[85] a) Z. Yuan, Y. Duan, H. Zhang, X. Li, H. Zhang, I. Vankelecom, *Energy Environ. Sci.* **2016**, *9*, 441 – 447; b) W. Lu, Z. Yuan, M. Li, X. Li, H. Zhang, I. Vankelecom, *Adv. Funct. Mater.* **2017**, *27*, 1604587; c) Y. Zhao, M. Li, Z. Yuan, X. Li, H. Zhang, I. F. J. Vankelecom, *Adv. Funct. Mater.* **2016**, *26*, 210 – 218.
[86] Z. Yang, R. Guo, R. Malpass-Evans, M. Carta, N. B. McKeown, M. D. Guiver, L. Wu, T. Xu, *Angew. Chem. Int. Ed.* **2016**, *55*, 11499 – 11502; *Angew. Chem.* **2016**, *128*, 11671 – 11674.
[87] M. Ali, B. Yameen, J. Cervera, P. Ramirez, R. Neumann, W. Ensinger, W. Knoll, O. Azzaroni, *J. Am. Chem. Soc.* **2010**, *132*, 8338 – 8348.
[88] a) F. Xia, W. Guo, Y. D. Mao, X. Hou, J. M. Xue, H. W. Xia, L. Wang, Y. L. Song, H. Ji, O. Y. Qi, Y. G. Wang, L. Jiang, *J. Am. Chem. Soc.* **2008**, *130*, 8345 – 8350; b) X. Hou, Y. J. Liu, H. Dong, F. Yang, L. Li, L. Jiang, *Adv. Mater.* **2010**, *22*, 2440 – 2443; c) X. Hou, F. Yang, L. Li, Y. L. Song, L. Jiang, D. B. Zhu, *J. Am. Chem. Soc.* **2010**, *132*, 11736 – 11742; d) W. Guo, Y. Tian, L. Jiang, *Acc. Chem. Res.* **2013**, *46*, 2834 – 2846; e) H. C. Zhang, X. Hou, L. Zeng, F. Yang, L. Li, D. D. Yan, Y. Tian, L. Jiang, *J. Am. Chem. Soc.* **2013**, *135*, 16102 – 16110; f) H. C. Zhang, Y. Tian, L. Jiang, *Chem. Commun.* **2013**, *49*, 10048 – 10063; g) H. C. Zhang, X. Hou, J. Hou, L. Zeng, Y. Tian, L. Li, L. Jiang, *Adv. Funct. Mater.* **2015**, *25*, 1102 – 1110; h) Z. Zhang, X. Sui, P. Li, G. Xie, X.-Y. Kong, K. Xiao, L. Gao, L. Wen, L. Jiang, *J. Am. Chem. Soc.* **2017**, *139*, 8905 – 8914.
[89] a) A. Andrieu-Brunsen, S. Micoureau, M. Tagliazucchi, I. Szleifer, O. Azzaroni, G. J. A. A. Soler-Illia, *Chem. Mater.* **2015**, *27*, 808 – 821; b) M. Ali, S. Nasir, P. Ramirez, J. Cervera, S. Mafe, W. Ensinger, *ACS Nano* **2012**, *6*, 9247 – 9257.
[90] F. M. Kievit, S. J. Florczyk, M. C. Leung, K. Wang, J. D. Wu, J. R. Silber, R. G. Ellenbogen, J. S. H. Lee, M. Q. Zhang, *Biomaterials* **2014**, *35*, 9137 – 9143.
[91] a) H. L. Kim, G. Y. Jung, J. H. Yoon, J. S. Han, Y. J. Park, D. G. Kim, M. Q. Zhang, D. J. Kim, *Mater. Sci. Eng. C* **2015**, *54*, 20 – 25; b) S. J. Florczyk, M. Leung, Z. S. Li, J. I. Huang, R. A. Hopper, M. Q. Zhang, *J. Biomed. Mater. Res. Part A* **2013**, *101*, 2974 – 2983; c) S. Jana, A. Cooper, M. Q. Zhang, *Adv. Healthcare Mater.* **2013**, *2*, 557 – 561; d) S. Jana, S. J. Florczyk, M. Leung, M. Q. Zhang, *J. Mater. Chem.* **2012**, *22*, 6291 – 6299.
[92] K. Wang, F. M. Kievit, S. J. Florczyk, Z. R. Stephen, M. Q. Zhang, *Biomacromolecules* **2015**, *16*, 3362 – 3372.
[93] S. W. Chen, Q. Zhang, T. Nakamoto, N. Kawazoe, G. P. Chen, *J. Mater. Chem. B* **2014**, *2*, 5612 – 5619.
[94] a) K. T. Gause, Y. Yan, J. W. Cui, N. M. O'Brien-Simpson, J. C. Lenzo, E. C. Reynolds, F. Caruso, *ACS Nano* **2015**, *9*, 2433 – 2444; b) Q. Dai, Y. Yan, C. S. Ang, K. Kempe, M. M. J. Kamphuis, S. J. Dodds, F. Caruso, *ACS Nano* **2015**, *9*, 2876 – 2885; c) J. W. Cui, R. De Rose, K. Alt, S. Alcantara, B. M. Paterson, K. Liang, M. Hu, J. J. Richardson, Y. Yan, C. M. Jeffery, R. I. Price, K. Peter, C. E. Hagemeyer, P. S. Donnelly, S. J. Kent, F. Caruso, *ACS Nano* **2015**, *9*, 1571 – 1580.
[95] X. C. Chen, K. F. Ren, J. H. Zhang, D. D. Li, E. Zhao, Z. J. Zhao, Z. K. Xu, J. Ji, *Adv. Funct. Mater.* **2015**, *25*, 7470 – 7477.
[96] Y. Lu, M. Ballauff, *Prog. Polym. Sci.* **2016**, *59*, 86 – 104.
[97] Q. Sun, Z. F. Dai, X. J. Meng, F. S. Xiao, *Chem. Soc. Rev.* **2015**, *44*, 6018 – 6034.
[98] Q. Sun, B. Aguila, J. Perman, N. Nguyen, S. Ma, *J. Am. Chem. Soc.* **2016**, *138*, 15790 – 15796.
[99] B. Zhang, C. Liu, L. J. Wang, X. F. Yi, A. M. Zheng, W. S. Deng, C. Z. Qi, F. J. Liu, *Catal. Commun.* **2015**, *68*, 25 – 30.
[100] J. Li, X. C. Wang, G. J. Chen, D. F. Li, Y. Zhou, X. N. Yang, J. Wang, *Appl. Catal. B* **2015**, *176*, 718 – 730.
[101] D. M. Dotzauer, J. H. Dai, L. Sun, M. L. Bruening, *Nano Lett.* **2006**, *6*, 2268 – 2272.
[102] L. Ouyang, D. M. Dotzauer, S. R. Hogg, J. Macanas, J. F. Lahitte, M. L. Bruening, *Catal. Today* **2010**, *156*, 100 – 106.
[103] Y. Y. Gu, I. Favier, C. Pradel, D. L. Gin, J. F. Lahitte, R. D. Noble, M. Gomez, J. C. Remigy, *J. Membr. Sci.* **2015**, *492*, 331 – 339.
[104] Z. J. Guo, X. C. Cai, J. Y. Xie, X. C. Wang, Y. Zhou, J. Wang, *Acs Appl. Mater. Interfaces* **2016**, *8*, 12812 – 12821.
[105] Q. Wang, X. C. Cai, Y. Q. Liu, J. Y. Xie, Y. Zhou, J. Wang, *Appl. Catal. B* **2016**, *189*, 242 – 251.
[106] W. Hou, Q. Wang, Z. J. Guo, J. Li, Y. Zhou, J. Wang, *Catal. Sci. Technol.* **2017**, *7*, 1006 – 1016.
[107] a) D. Puppi, C. Migone, A. Morelli, C. Bartoli, M. Gazzarri, D. Pasini, F. Chiellini, *J. Bioact. Compat. Polym.* **2016**, *31*, 531 – 549; b) J. Malda, J. Visser, F. P. Melchels, T. Jungst, W. E. Hennink, W. J. A. Dhert, J. Groll, D. W. Hutmacher, *Adv. Mater.* **2013**, *25*, 5011 – 5028; c) R. L. Truby, J. A. Lewis, *Nature* **2016**, *540*, 371 – 378.
[108] L. Zhang, L.-H. Cai, P. S. Lienemann, T. Rossow, I. Polenz, Q. Vallmajo-Martin, M. Ehrbar, H. Na, D. J. Mooney, D. A. Weitz, *Angew. Chem. Int. Ed.* **2016**, *55*, 13470 – 13474; *Angew. Chem.* **2016**, *128*, 13668 – 13672.
[109] a) L. Kou, T. Huang, B. Zheng, Y. Han, X. Zhao, K. Gopalsamy, H. Sun, C. Gao, *Nat. Commun.* **2014**, *5*, 3754; b) X. X. Meng, S. L. Perry, J. D. Schiffman, *ACS Macro Lett.* **2017**, *6*, 505 – 511; c) H. Q. Ma, G. K. Chen, J. N. Zhang, Y. Liu, J. Nie, G. P. Ma, *Polymer* **2017**, *110*, 80 – 86.
[110] a) S. Ghasimi, S. Prescher, Z. J. Wang, K. Landfester, J. Yuan, K. A. I. Zhang, *Angew. Chem. Int. Ed.* **2015**, *54*, 14549 – 14553; *Angew. Chem.* **2015**, *127*, 14757 – 14761; b) S. Fischer, J. Schmidt, P. Strauch, A. Thomas, *Angew. Chem. Int. Ed.* **2013**, *52*, 12174 – 12178; *Angew. Chem.* **2013**, *125*, 12396 – 12400.

Manuscript received: October 4, 2017
Accepted manuscript online: November 9, 2017
Version of record online: April 26, 2018

